Mon. Not. R. Astron. Soc. **000**, 1–21 (2002) Printed 5 February 2008 (MN LATEX style file v2.2)

Surface density profiles of collisionless disc merger remnants

Thorsten Naab[1,2⋆] and Ignacio Trujillo[3,4]
[1] *Insitute of Astronomy, Madingley Road, Cambridge, CB3 0HA, UK*
[2] *Universitäts-Sternwarte München, Scheinerstr. 1, D-81679 Münc hen,Germany;*
[3] *Max-Planck-Institut für Astronomie, Königstuhl 17, Heidelberg D-69117, Germany*
[4] *School of Physics and Astronomy, University of Nottingham, University Park, Nottingham NG7 2RD, UK*

Accepted ???. Received ??? in original form ???

ABSTRACT
We present a detailed surface density analysis of a large sample of simulated collisionless mergers of disc galaxies with bulges (mass ratios 1:1, 2:1, 3:1, 4:1, and 6:1) and without bulges (mass ratios 1:1 and 3:1). A dissipative component was not included. The randomly projected remnants were fit with a single Sérsic function and a Sérsic function plus an exponential. They were classified, according to their bulge–to–total (B/T) ratio, either as a one-component system or as a two-component systems. In general projection effects change the classification of a remnant. Only merger remnants of discs with bulges show properties similar to observed early–type galaxies. Their B/T ratios are in the range $0.2 < B/T < 1$. Surprisingly, the initial mass ratio has a weak influence on the distributions of B/T, effective radius and Sérsic index n. For all one-component projections ($\approx 60\%$ of all projections) the Sérsic index distribution peaks at $3 < n < 4$. However, the mass ratio is tightly linked to the properties of the outer exponential components which resemble pressure supported, spheroidal halos for 1:1 and 2:1 remnants and elongated heated discs for 6:1 remnants. We found distinct correlations between the fitting parameters which are very similar to observed relations (e.g. larger bulges have lower effective surface densities). No indications for a correlation between the surface density profiles and other global parameters like remnant masses, isophotal shapes or central velocity dispersions are found. The remnants have properties similar to giant elliptical galaxies in the intermediate mass regime. A binary disc merger origin for all early-type galaxies, especially the most massive ones, is unlikely. Observed nearby merger remnants have properties similar to the simulated remnants. They can have formed from binary disc mergers and might evolve into early–type galaxies within a few Gyrs.

Key words: methods:numerical – methods: N-body simulations – galaxies: elliptical and lenticular, cD – galaxies: formation – galaxies: evolution – galaxies: fundamental parameters

1 INTRODUCTION

For many decades the surface brightness profiles of elliptical galaxies have been considered to be well described by the de Vaucouleurs (1948) $r^{1/4}$-profile. However, from the early 1990's, as the quality of photometric data improved, it became clear that the de Vaucouleurs law is not valid over the whole observable radius range and it became necessary to use a fitting function which can account for variations in the curvature of the light profile (Capaccioli 1987; Davies et al. 1988; Caon et al. 1993; Burkert 1993). Following these pioneering works, several authors have showed that the surface brightness profiles of elliptical galaxies are better described by the Sersic (1968) $r^{1/n}$-profile. This is not surprising as the shape parameter n of the Sérsic function is an additional fitting parameter. Interestingly, n is strongly correlated with other observed global properties of elliptical galaxies derived independently of the $r^{1/n}$ fits, such as: total luminosity, effective radius, (Caon et al. 1993; Young & Currie 1994, 1995; Jerjen & Binggeli 1997; Prugniel & Simien 1997), central velocity dispersion (Graham et al. 2001; Vazdekis et al. 2004), and also the masses of super-massive black holes (Graham et al. 2001). The non–homology of elliptical galaxies has also been shown to account for a large fraction of

⋆ E-mail: naab@usm.lmu.de

the tilt of the Fundamental Plane (Trujillo et al. 2004). In general, more massive giant ellipticals have more concentrated light profiles indicated by larger values of n which is most likely a direct consequence of the formation process. Recently, de Jong et al. (2004) have performed a two component decomposition (inner Sérsic and outer exponential "disc") of a large sample of 558 early–type galaxies. They found strong evidence for outer exponential components in early–type galaxies at all luminosities. However, as they have pointed out, it was not possible to prove without further information about kinematics and stellar populations whether this analysis has any physical significance. In particular it was not clear whether the exponential component represented a classical flattened, rotationally supported thin or thick disc. If the exponential components turn out to be real de Jong et al. (2004) found possibly meaningful correlations between the fitting parameters such as: bulge sizes and disc sizes; bulge-to-disc ratio, bulge shape parameter, and bulge effective radius.

It is the aim of this paper to test the significance of binary disc mergers for the formation and evolution of early–type galaxies and bulges by investigating the surface density profiles of the merger remnants. As our progenitor discs have properties similar to present day disc galaxies a simulated merger remnant will not resemble a present day early–type in the sense that its stellar population is too young. The distribution and kinematics of the stars, however, might be in agreement. If the discs have merged early enough, $z \gtrsim 1$, having similar properties (and there are indications for the existence of large scale discs at high redshift, see e.g. Labbé et al. 2003) their stellar populations might have evolved into early–type populations by now (discs might on average have been smaller in the past but our models are scale-free) and a comparison to the properties of present day early–type galaxies, as mentioned above, is justified. On the other hand with a direct comparison to observed present day merger remnants we can test whether nearby merger remnants originate from discs and whether they will evolve into early–type galaxies in the future.

Such a sample has been published by Rothberg & Joseph (2004) who have successfully fitted Sérsic-profiles to surface brightness profiles of 51 observed merger remnants. They conclude that the remnants might evolve into ellipticals as they can have (K-band) luminosities in the range of an L^* elliptical and photometric properties that are in principal similar to observed ellipticals. Most of the remnants have Sérsic indices between $1 < n < 6$ with a peak at $n = 2$. They find indications for more concentrated profiles, $n > 8$ for some remnants. However, there are still some open questions, e.g. they do not find a correlation of the shape parameter with luminosity or isophotal shape (most of the remnants have discy isophotes) and a kinematical investigation is still missing and at present it seems still difficult to argue that present disc merger remnants evolve into bona fide early–type galaxies based on observations alone.

On the theoretical side it is now almost 30 years that it has been proposed that elliptical galaxies might form from mergers of disc galaxies. As an alternative to the even older monolithic collapse scenario the 'merger hypothesis' became more and more popular in the framework of cosmological models where structure forms hierarchically by mergers and every galaxy is expected to have experienced at least one (maybe more) major merger during its lifetime. The first numerical experiments in the early 1970s have been followed by more and more self-consistent collisionless major merger models of disc galaxies (see Naab & Burkert 2003 and references therein). As pure disc galaxies have much lower central phase-space densities than ellipticals it has been argued for a long time that one can not make elliptical galaxies by collisionless mergers of pure discs (Ostriker 1980; Carlberg 1986). However, Hernquist (1993b) "solved" this problem by adding sufficiently massive concentrated bulge components to the progenitor galaxies. The surface density profiles of the merger remnants have been compared to a de Vaucouleurs $r^{1/4}$-profile and a reasonable agreement has been found (Barnes 1992; Hernquist 1992, 1993b). Naab & Burkert (2003) have found a good statistical agreement between observations of intermediate mass giant ellipticals and simulations mergers of discs with varying mass-ratios with respect to kinematic and photometric properties including the isophotal shape. The most characteristic change with mass ratio is the amount of rotation of the remnants. Equal mass remnants are slowly rotating whereas unequal mass remnants are in general fast rotators (Barnes 1998; Naab et al. 1999; Naab & Burkert 2003). There are, however, disagreements in the higher order moments of the line-of-sight velocity distributions for fast rotating remnants (Naab & Burkert 2001b). Orbital analysis of merger remnants has shown that equal mass remnants are dominated by box orbits whereas unequal mass remnants are dominated by tube orbits (see Jesseit et al. 2005, and references therein). As the stellar orbits are the backbones of elliptical galaxies a different orbital content might lead to different projected surface density profiles.

A statistical analysis of the surface density profiles of merger remnants has not been performed so far. Given the observational evidence that the Sérsic-function provides a better fit to observed ellipticals, we decided to investigate the surface density profiles of collisionless disc merger remnants in more detail and to probe whether the profiles of the simulated galaxies are well described by a Sérsic function or if they can be decomposed in a Sérsic part and a part with an exponential profile (here called "disc" for convenience) and whether the observed relations between the structural parameters can be recovered. Only recently, some groups have used the Sérsic-function to fit simulated merger remnants. González-García & Balcells (2005) found that merger remnants of disc galaxies with massive bulges are more concentrated than pure disc mergers. Bournaud et al. (2004) realized that the outer parts of remnants with mass ratios larger than 4:1 can show an exponential surface density profile similar to a disc galaxy.

In this paper we present the detailed application of an observational analysis method (Trujillo et al. 2001; Aguerri & Trujillo 2002) for surface brightness profiles of early–type galaxies to the projected surface density profiles of simulated galaxies. The profiles are fitted with a pure Sérsic and a Sérsic + exponential profile taking the full photometric information into account (e.g. seeing, ellipticities, and errors). This enables us to perform a self-consistent disc + bulge decomposition. In a first step, the analysis is applied to a statistical set of simulated collisionless merger remnants of progenitor disc galaxies with bulges and mass ratios of 1:1,

2:1, 3:1, 4:1, and 6:1 and bulge-less progenitors with mass ratios of 1:1 and 3:1, for comparison.

The paper is structured as follows: In Section 2 we review the parameters of the simulations used. The surface density analysis is described in detail in Section 3 with an exemplary application to the initial conditions and individual simulated merger remnants shown in the appendix. In Section 4 we present the results based on the whole sample. The resulting parameter relations are discussed separately in Section 5. In Section 6 we investigate the nature of the outer exponential component and in Section 7 we summarise and discuss the results.

2 SIMULATION PARAMETERS

The statistical set of merger simulations of disc galaxies with mass ratios of 1:1, 2:1, 3:1 and 4:1 is described in detail in Naab & Burkert (2003). Here we only give a brief summary. We used the following system of units: gravitational constant G=1, exponential scale length of the larger disc $h = 1$ and mass of the larger disc $M_d = 1$. Each galaxy consists of an exponential disc, a spherical, non-rotating bulge with mass $M_b = 1/3$, a Hernquist density profile (Hernquist 1990) with a scale length $a_b = 0.2h$ and a spherical pseudo-isothermal halo with a mass $M_h = 5.8$, cut-off radius $r_c = 10h$ and core radius $\gamma = 1h$ (Hernquist 1993a). The equal-mass mergers were calculated adopting in total 400000 particles with each galaxy consisting of 20000 bulge particles, 60000 disc particles, and 120000 halo particles. The low-mass companion contained a fraction of $1/\eta$ (mass ratio $\eta = 1/1$, 2/1, 3/1, 4/1 and 6/1) the mass and the number of particles in each component with a disc scale length of $h = \sqrt{1/\eta}$, as expected from the Tully-Fisher relation (Pierce & Tully 1992). The galaxies approached each other on nearly parabolic orbits (in agreement with estimates from cosmological simulations (Khochfar & Burkert 2006)) with an initial separation of $r_{sep} = 30$ length units and a pericenter distance of $r_p = 2$ length units. The initial parameters for the disc inclinations were selected in an unbiased way following the procedure described by Barnes (1998). We have realized 16 different initial orientations resulting in 16 equal-mass remnants and 32 remnants for every higher mass ratio, respectively (see Tbl. 1 in Naab & Burkert 2003). In addition, we have rerun the merger simulations with mass ratios of 1:1 and 3:1 with bulge-less progenitor discs. This resulted in 192 simulated merger remnants that are investigated in this paper.

All simulations have been performed using the tree-code VINE (Wetzstein et al., in preparation) in combination with the GRAPE-5/6 special purpose hardware (Kawai et al. 2000). The Plummer-softening for the force calculation was set to $\epsilon = 0.05$. Time integration was performed with a with a Leap-Frog integrator with a fixed time-step of $dt = 0.04$. For further details on the simulations see Naab & Burkert (2003).

3 ANALYSIS OF THE SURFACE DENSITY PROFILE AND CLASSIFICATION

In the classical view the surface brightness profiles of elliptical galaxies have been assumed to follow the de Vaucouleurs $r^{1/4}$-profile (de Vaucouleurs 1948)

$$I(r) = I(0)e^{-7.67(r/r_e)^{1/4}}. \quad (1)$$

$I(0)$ is the central surface brightness, r_e is semi-major axis effective radius and the factor 7.67 is chosen such that the effective radius encloses half the total luminosity of the galaxy. In this paper we use the Sérsic-function (Sersic 1968) to fit the surface density profile of simulated merger remnants. The Sérsic-function is a generalized version of the de Vaucouleurs-profile allowing the exponent to account for the varying curvature of the surface brightness profiles of observed galaxies. As we have shown in Sec. 1 there is strong evidence that the curvature of the light profile is a physically meaningful parameter which is closely linked to other properties of ellipticals. Throughout the paper we assume that the surface density of the simulated merger remnants reflect their surface brightness with a constant mass–to–light ratio along the radial profile. The Sérsic-function can be written as

$$I(r) = I(0)e^{-b_n(r/r_e)^{1/n}}. \quad (2)$$

The three free parameters (which is one more than for the de Vaucouleurs-profile) are: the central surface brightness $I(0)$, the effective radius r_e, and the shape parameter n, the so called Sérsic-index. The factor b_n is a function of the shape parameter n, and is chosen such that the effective radius encloses half of the total luminosity. The exact value is derived from $\Gamma(2n)=2\gamma(2n,b_n)$, where $\Gamma(a)$ and $\gamma(a,x)$ are the gamma and the incomplete gamma functions. In case of $n = 1$ the profile is exponential and in case of $n = 4$ the profile is de Vaucouleurs.

To systematically analyse the simulated merger remnants we created artificial images of every remnant seen from 100 random projections by binning the central 10 length units into 128×128 pixels. For the simulation parameters given above this resulted in 14400 images for mergers with bulges and 4800 for mergers without bulges in the progenitor galaxies. In an automated procedure every image was smoothed with a Gaussian filter of standard deviation 0.05 length scales. The surface density profile, the isophotes and their best fitting ellipses were determined using a data reduction package kindly provided by Ralf Bender. The surface density profile was thereafter fitted as described below using the algorithm presented in Trujillo et al. (2001) and Aguerri & Trujillo (2002). As the Sérsic-function fit is sensitive to the detailed shape in the innermost regions of the surface density profiles we followed a conservative approach and excluded all data points at radii $r_{fit} < 0.1$ (≈ 2 softening lengths) which might be affected by the numerical force softening. However, using slightly smaller or larger values for r_{fit} did not change the global results.

In addition to the fit of a single Sérsic-function to the surface density profiles we performed a decomposition (usually called "bulge-disc decomposition") allowing for a bulge component described by a Sérsic-function and an exponential component like in disc galaxies (Freeman 1970):

$$I(r) \quad = \quad I_{Disc}(r) + I_{Bulge}(r)$$

$$= I_D(0)\exp(r/h_D) + I_B(0)e^{-b_n(r/r_{eB})^{1/n_B}}. \quad (3)$$

The meaning of the structural parameters of the bulge component are the same as those described for the Sérsic only model. $I_D(0)$ is the central surface density and h_D is the scale length of the exponential component. The set of free parameters is completed with the ellipticities of the bulge ϵ_B and the disc ϵ_D. To avoid confusion with the observational notation all surface densities that result directly from the simulated remnants are denoted by Σ in the following. We have to note at this point that an exponential profile alone does not prove the existence of a disc component which in addition has to be flattened and supported by rotation. In Section 6 we will show that some remnants have exponential components that are not discs. For convenience we keep the notation "disc" for the exponential component as long as there is not other evidence than the profile shape.

To quantify which fraction of mass corresponds to the bulge and which fraction corresponds to the disc we used the bulge–to–total (B/T) ratio. B is the projected bulge mass and $T = B+D$ is the total mass (here D is the disc mass) of the system. Using the parameter values obtained from the fit we estimated B/T according to:

$$\frac{B}{T} = \frac{I_B(0)r_{eB}^2(n_B/b_n^{2n_B})(1-\epsilon_B)\Gamma(2n_B)}{I_B(0)r_{eB}^2(n_B/b_n^{2n_B})\Gamma(2n_B)(1-\epsilon_B) + I_D(0)h_D^2(1-\epsilon_D)} \quad (4)$$

where $\Gamma(a)$ is the gamma function. The frequently used bulge–to–disc ratio, B/D, is then given by

$$B/D = \frac{B/T}{1-B/T}. \quad (5)$$

In some rare cases (below 2%) the application of Eqn. 4 directly using the parameters of the fit caused problems. For example, if the fitted central surface density of the exponential scale component is below the outermost measured value of the remnant and the scale length h_D becomes unrealistically large (i.e. larger than the size of the remnant containing 95% of all the particles), we would significantly overestimate the disc mass and underestimate B/T. For these cases we assumed $B/T = 1$.

The size of the BD systems was estimated by computing the global semi-major effective radius, r_{eG}, solving the equation

$$\frac{B/T}{1-B/T}\left[1-\frac{2\gamma(2n, b_n(r_{eG}/r_{eB})^{1/n})}{\Gamma(2n)}\right] = 2\gamma(2, r_{eG}/h_D) - 1. \quad (6)$$

A BD–decomposition of the merger remnants allowed us to classify the surface density profiles in two categories depending on the bulge–to–total (B/T) ratios. Projections with $B/T > 0.7$ were considered pure bulge systems and, for simplicity reasons, the structural parameters determined from the Sérsic-only fits were used. Projections with $B/T < 0.7$ were considered two-component disc+bulge systems. For all cases we compared the reduced chi–squared of the Sérsic–only fit and the BD–decomposition fit. In general the fit was considered sufficiently accurate if the reduced chi–squared value of the fit was smaller than unity. For those cases where both fits resulted in a reduced chi–squared value smaller than unity (see for example second row in Fig. A10) we computed the probability

$$P(\chi^2|\nu) = \gamma\left(\frac{\nu}{2}, \frac{\chi^2}{2}\right) \quad (7)$$

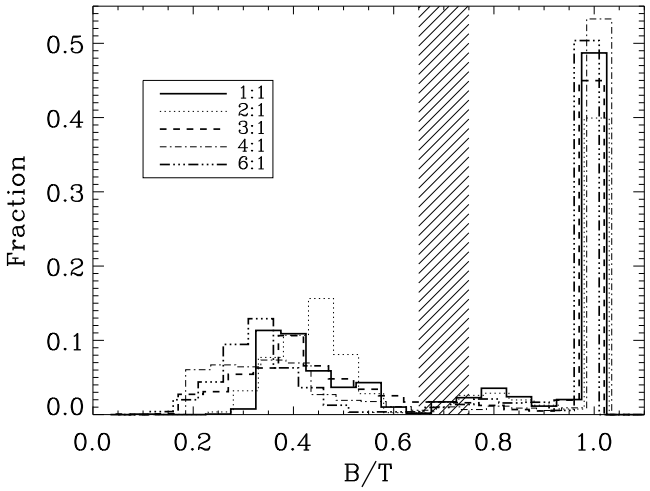

Figure 1. Histogram of the bulge–to–total ratios (B/T) for all projected 1:1, 2:1, 3:1, 4:1, and 6:1 merger remnants. The shaded area indicates the transformation region around $B/T \approx 0.7$ between disc+bulge systems and pure bulge systems. The curves are slightly shifted for better visibility.

that the chi–squared value is due to chance (Press et al. 1992). Here γ is the incomplete gamma function and ν is the number of degrees of freedom. If that probability for the Sérsic-only fit was smaller than $P < 0.32$ the fit was considered as sufficiently accurate and the projected remnant was classified as one component with $B/T = 1$. Changing the threshold probability to $P = 0.5$ or $P = 0.2$ does not change the results.

As it is the aim of this study to investigate the statistical properties of the remnants we apply identical boundary conditions like weights, computation of errors etc. to all projected images even if fine-tuning might reduce the residuals slightly in one or the other case.

A potential source of concern for fitting a bulge and a disc to the surface brightness distribution of the galaxies is the degeneracy of the solution. In fact, if the fit is doing blindly, the algorithm would try, in some cases, to accommodate the exponential component fitting the inner regions of the profile. To avoid this our code selects an initial guess for the exponential component that guaranteed that the outer observable points are well described by this component in the first step of the iteration. Even so, it could be possible that the final solution of the fit would provide an answer where the inner points of the surface brightness were described primarily by the exponential component. To avoid these cases, the algorithm checks whether the central intensity of the fitted exponential component is larger than the central intensity of the fitted Sérsic component. If this is the case the fit starts again changing the initial conditions until a proper fit is achieved. This guarantees that the Sérsic component is always describing the inner regions of the profile and that B/T is meaningful.

4 STATISTICAL ANALYSIS

In the appendix we show a detailed analysis of the initial conditions and individual examples of merger remnants. As

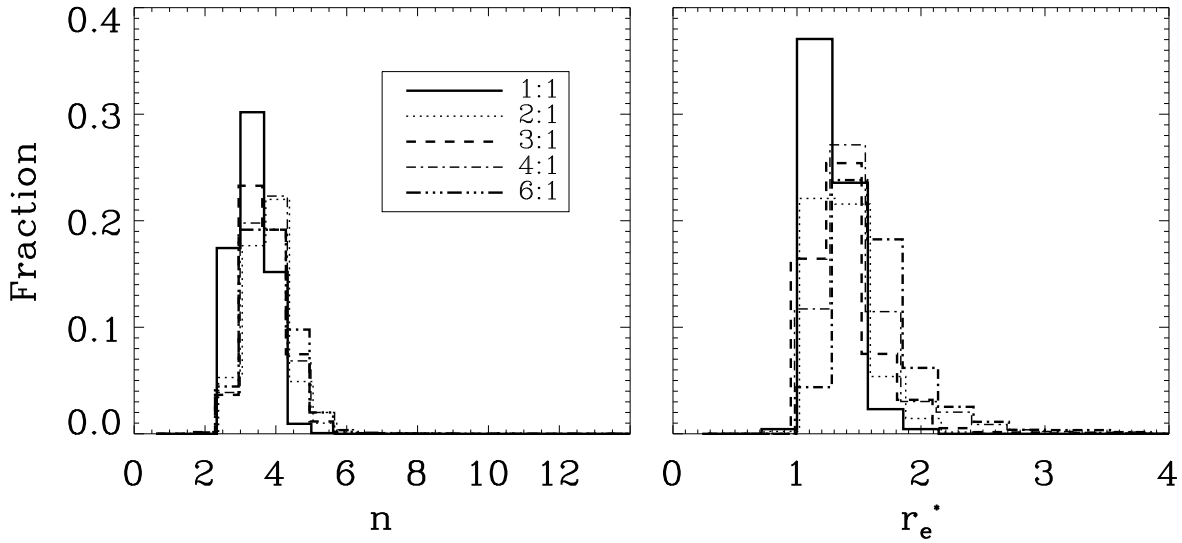

Figure 2. Distribution of properties for all projections classified as pure bulges for the projected 1:1, 2:1, 3:1, 4:1, and 6:1 merger remnants. The data are shown as a fraction of all projected remnants at a given mass ratio. *Left*: The Sérsic-index n. The distributions show a weak dependence on mass-ratio and peak at around $3 < n < 4$. *Right*: Effective radii which peak at $1 < r_e^* < 1.7$ for all mass ratios. *Right*:

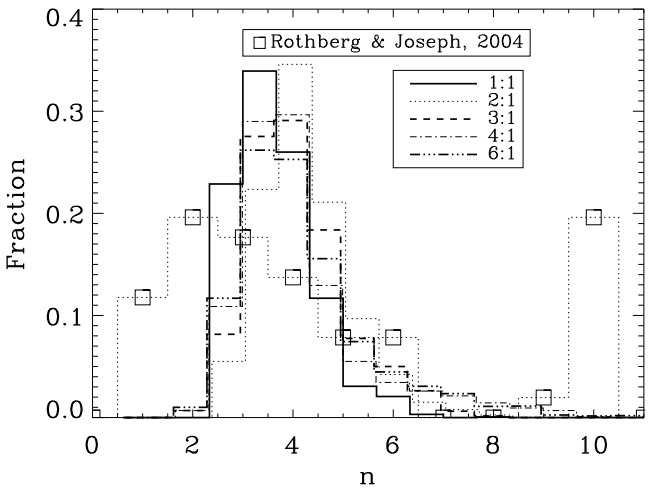

Figure 3. Histogram of the Sérsic-index n for all projections. In contrast to Fig.2 we have plotted all results from the Sérsic only fit independent of the classification (e.g. B/T) of the projection. The distributions peak at similar values but show a tail towards larger values of n. The observed (normalised) distribution of local merger remnants (Rothberg & Joseph 2004) is indicated by open squares.

we show there the properties of the merger remnants depend strongly on the respective projection angle under which the remnant would be observed. In this section we present the results of a statistical analysis of all merger remnants, with and without bulges in the progenitor discs, by analysing 100 random projections of every merger remnant grouped according to their mass ratios. The results for mergers with bulges are summarized in Tab. 1.

Table 1. Photometric properties (see Figs. 1 - 4) for mergers with bulges for different mass ratios with 1σ deviations.

Mass ratio	1:1	2:1	3:1	4:1	6:1
n	3.1	3.56	3.60	3.66	3.66
±	0.51	0.59	0.62	0.66	0.72
r_e^*	1.19	1.27	1.36	1.47	1.60
±	0.16	0.23	0.31	0.43	0.51
r_{eG}	1.15	1.09	1.11	1.16	1.20
±	0.08	0.09	0.10	0.08	0.1
n_B	1.70	1.70	1.66	1.39	1.32
±	0.33	0.25	0.56	0.41	0.48
r_{eB}	0.42	0.38	0.39	0.33	0.33
±	0.09	0.07	0.19	0.11	0.15
h_D	1.32	1.29	1.22	1.18	1.19
±	0.24	0.20	0.29	0.29	0.18

4.1 Progenitors with bulges

In Fig. 1 we show the bulge–to–total (B/T) ratios for all merger remnants with bulges and mass ratios of 1:1, 2:1, 3:1, 4:1, and 6:1. The transition region from bulge+disc systems to pure bulge systems around $B/T = 0.7$ is indicated by the shaded area. Small changes of this threshold value would not influence the global results as all mass ratios show a minimum number of projections in the transition region. Fig. 1 shows that merging increases the bulge fraction of the galaxy significantly. For comparison, the B/T values of the initial disc do not exceed $B/T = 0.20$ (see appendix). The B/T ratios for every mass ratios cover a wide range from $0.2 < B/T < 1$ and the distributions are remarkably similar. For every mass ratio we would identify pure bulge

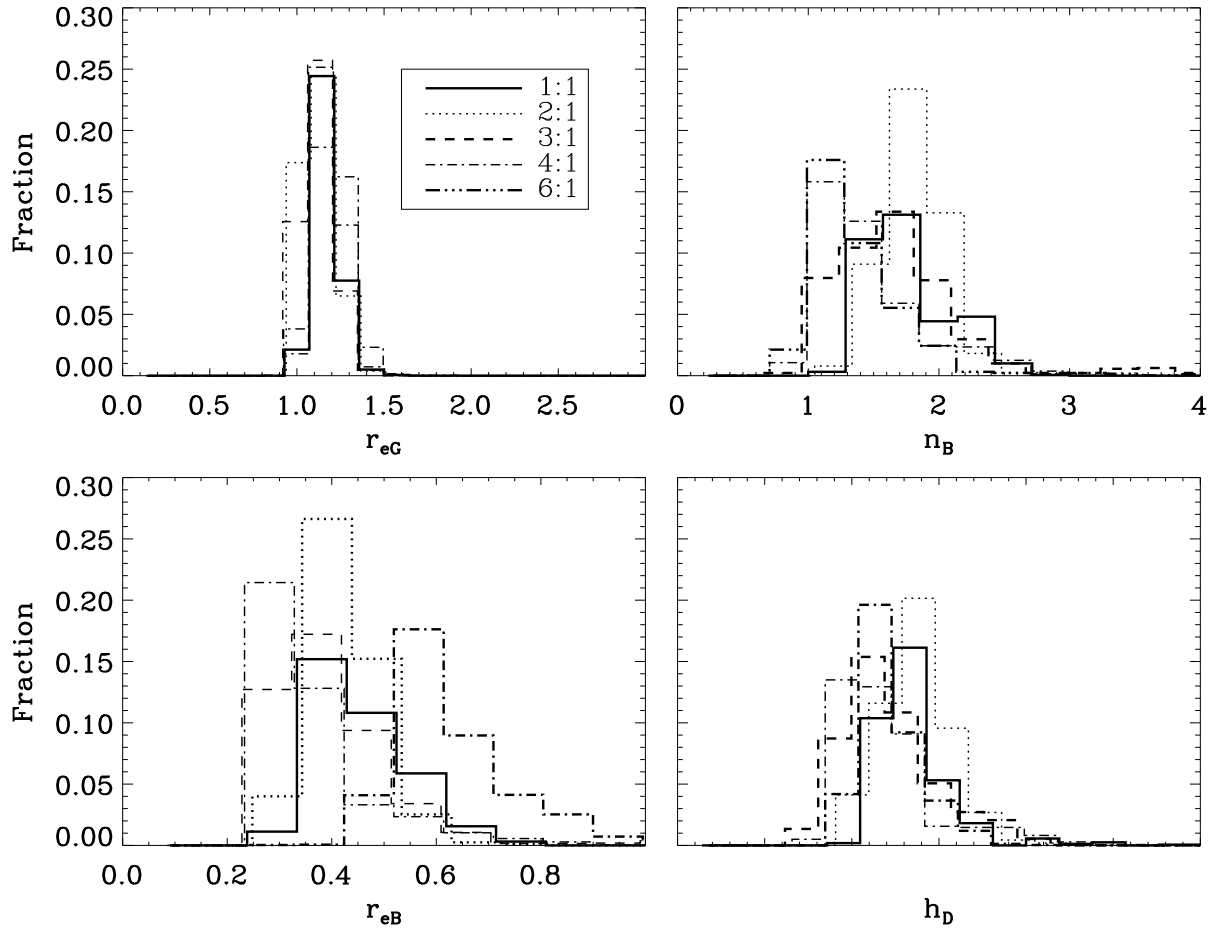

Figure 4. Distribution of the properties for the projections classified as D/B systems for all mass ratios. *Upper left*: effective sizes; *Upper right*: Sérsic-indices of the bulge components; *Lower left*: Effective radii of the bulge components; *Lower right*: Scale lengths of the exponential components.

systems as well as bulge+disc systems. Using $B/T = 0.7$ as the division line the percentage of pure bulge systems would be 66% for the 1:1, 51% for the 2:1, 54% for the 3:1, 58% for the 4:1, and 58% for the 6:1 remnants, respectively. 1:1 remnants have the largest number of projections which would be classified as pure bulges. There is no trend for remnants with mass ratios of 2:1 and higher to be less dominated by bulge-only projections, e.g. 6:1 merger remnants do not have significantly more projections classified as disc+bulge systems as e.g. 2:1 remnants. However, there is a trend that high mass-ratio remnants classified as BD can have lower B/T indicating that the exponential component is becoming more dominant.

In the following we focus on the properties of the projections classified as pure bulge systems with $B/T > 0.7$ (the distributions in Figs. 1 - 6 are shown as fractions of all projected remnants at a given mass ratio). The distribution of the best fitting Sérsic-indices for the five mass ratios is shown in Fig. 2. The distributions are very similar for all mass ratios and peak between $3 < n < 4$. The bulk of the projections lie in the range $2.5 < n < 6$ which is in general in good agreement with observed values of intermediate mass giant elliptical galaxies (e.g. Vazdekis et al. 2004; Trujillo et al. 2004; de Jong et al. 2004, and references therein). Ellipticals with $M_B > -18$ have on average smaller shape parameters, massive ellipticals with $M_B < -20$ and large velocity dispersions have on average shape parameters $n > 4$. This is demonstrated in Fig. 5 where show the mean values of the shape parameters and the effective radii in comparison to a sample of elliptical galaxies (Peletier et al. 1990; Caon et al. 1990, 1994; Binggeli & Jerjen 1998; Gutiérrez et al. 2004). The numerical simulations are scale free and can therefore be shifted to smaller as well as larger sizes along the shaded region. We have assumed a scaling of 3kpc for the initial disc scale length which is in best agreement with observations. Ellipticals with larger shape (smaller) parameters which are in general also more massive (less massive) can not be fitted by our merger remnants. Interestingly, our distributions of the shape is very similar to the distributions of dark matter halos in cosmological simulations (Merritt et al. 2005).

For a better comparison with the sample of local merger remnants by Rothberg & Joseph (2004) who fitted only Sérsic profiles we show in Fig. 3 the distribution of the indices for the Sérsic only fit for every projection independent of its B/T value. The simulated distributions peak at similar values and now have a prominent tail towards larger values

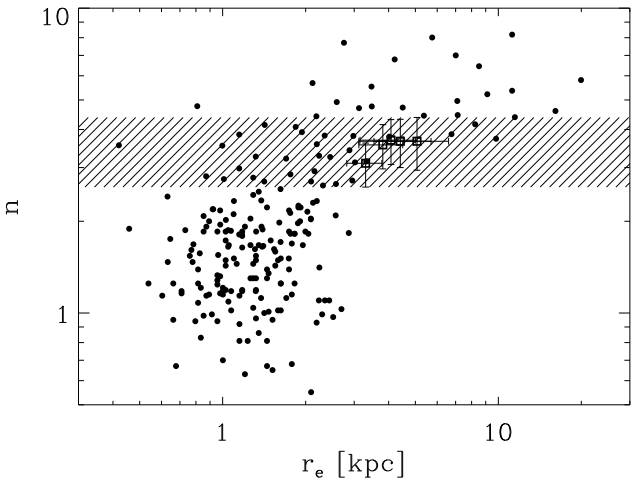

Figure 5. Distribution of effective radius r_e^* versus shape parameter n for the simulated merger remnants at different mass ratios (symbols with error bars from Tab. 1)and a sample of observed (dots) elliptical galaxies (Peletier et al. 1990; Caon et al. 1990, 1994; Binggeli & Jerjen 1998; Gutiérrez et al. 2004). We have assumed an initial disc scale length of 3kpc for a good agreement with the data. However, the simulations are scale free and can be shifted horizontally along the shaded area.

of n. The distribution is similar to the local merger remnants from Rothberg & Joseph (2004). However, we are missing all projections with $n \leqslant 1$ and the observed distribution peaks at lower n ($n = 2$). This might reflect the fact that some progenitors had less massive bulges resulting in smaller values of n (see Section 4.2). We also find indices larger than $n = 8$ for mass ratios 4:1 and 6:1. Rothberg & Joseph (2004) have suggested that these values result from excess light at the center. In our case it is those remnants that show a concentrated bulge plus a very clear exponential component and were classified as two-component systems.

Comparing to previous simulations González-García & Balcells (2005) have found values between $3 < n < 8$ (they only performed Sérsic-fits) for a small set of 1:1, 2:1 and 3:1 remnants which is in good agreement with our results in this mass-ratio range taking into account that their initial bulge was more massive (the bulge-to-disc ratio was 1/2). In addition, they also found no dependence of n on the mass-ratio.

The distribution of the effective radii for the systems classified as pure bulges $B/T > 0.7$ is shown in Fig. 2. To correct for the flattening we computed the circularised effective radius $r_e^* = r_e\sqrt{1-\epsilon}$ using the semi-major axis effective radius r_e and the ellipticity, ϵ, of the image. The distributions for all mass-ratios are similar and peak at $1 < r_e^* < 1.7$ with a tail extending to values as large as $r_e^* = 3$. Compared to the initial conditions the photometric sizes do, on average, not or only weakly increase. This result seems at first surprising, however it was already found by Hernquist (1993b) that the half-mass radius of the remnant can be of a similar size than the initial disc. For a direct comparison we have computed the projected half mass radius of one of our runs that is identical to "1-nrb" in Hernquist (1993b). In three different projections our values (1.80,1.2,1.15) are similar to theirs (1.92, 1.31, 1.18) taking into account that we have 4-5 times more particles for the luminous components and 7 times more particles in the halo component.

We will now focus on all projected remnants that are classified as disc+bulge systems (Fig. 4). In the upper left we show the distribution of the global effective radii as they have been calculated using Eqn. 6. All remnants classified as DB systems have similar sizes of $r_{eG} \approx 1.2$, similar to the initial conditions. Consequently, independent of B/T and the initial mass-ratio all remnants have similar sizes than the initial discs. The distribution of the Sérsic-indices and the effective radii of the bulge components of the BD fits are shown in the upper right of Fig. 4. The Sérsic-indices for the bulge components of 1:1, 2:1 and 3:1 remnants peak at values of $n_B = 1.8$. For 4:1 and 6:1 remnants the distributions peak at slightly lower values around $n_B = 1.1$ with tail of higher values extending to $n_B = 2.8$. The effective radii peak around $0.2 < r_{eB} < 0.8$ for all mass-ratios. The maximum values are about a factor four larger than the effective radius of the bulge component when analysed for the initial conditions. The scale lengths of the fitted disc components peak around $1.2 < h_D < 1.3$ which is about 30% larger than the initial disc scale lengths (Fig. 4)

4.2 Bulge-less progenitors

We have re-simulated the mergers with mass ratios 1:1 and 3:1 using progenitor discs without bulge components to investigate the influence of the bulge on the surface density profile of the merger remnant.

In the upper panel of Fig. 6 we show the result for the distribution of B/T-ratios of the projected remnants. The result is significantly different to the analysis of the remnants with bulge (see Fig. 1). Most projected remnants are classified as two-component systems. The distributions peak at $B/T = 0.5$ for the equal-mass remnants and $B/T = 0.35$ for the 3:1 remnants, almost reflecting the mass-ratios of the progenitor discs. From the lower two panels in Fig. 6 it becomes clear that the systems classified as pure bulges have $1.2 < n < 2.5$ and therefore very shallow surface density profiles and, if the system is classified as a two component system, the Sérsic index of the bulge is smaller than one.

Interestingly, Sérsic indices as small as $n = 1$ have been observed for local merger remnants (Rothberg & Joseph 2004) which might indicate that some progenitor discs did not have prominent stellar bulges (or bulges with low concentration).

For a similar set of simulations González-García & Balcells (2005) fitting a Sérsic only model for all remnants find a range of $2.4 < n < 3.2$. There might be two origins for this discrepancy: all our remnants that appear more concentrated show a two component structure and were not classified as one component systems. If we limit ourselves to Sérsic fits only like González-García & Balcells (2005) the indices would be in the range $1.2 < n < 3.1$. The fact that we find smaller values for n might be caused by the different choice of initial conditions for the discs. González-García & Balcells (2005) use a truncated exponential disc which leads to remnant profiles that can not be fitted properly in the outer parts. Our remnants show very exponential profiles in the outer parts which are fitted with small residuals leading to smaller over all values of n. Despite the differ-

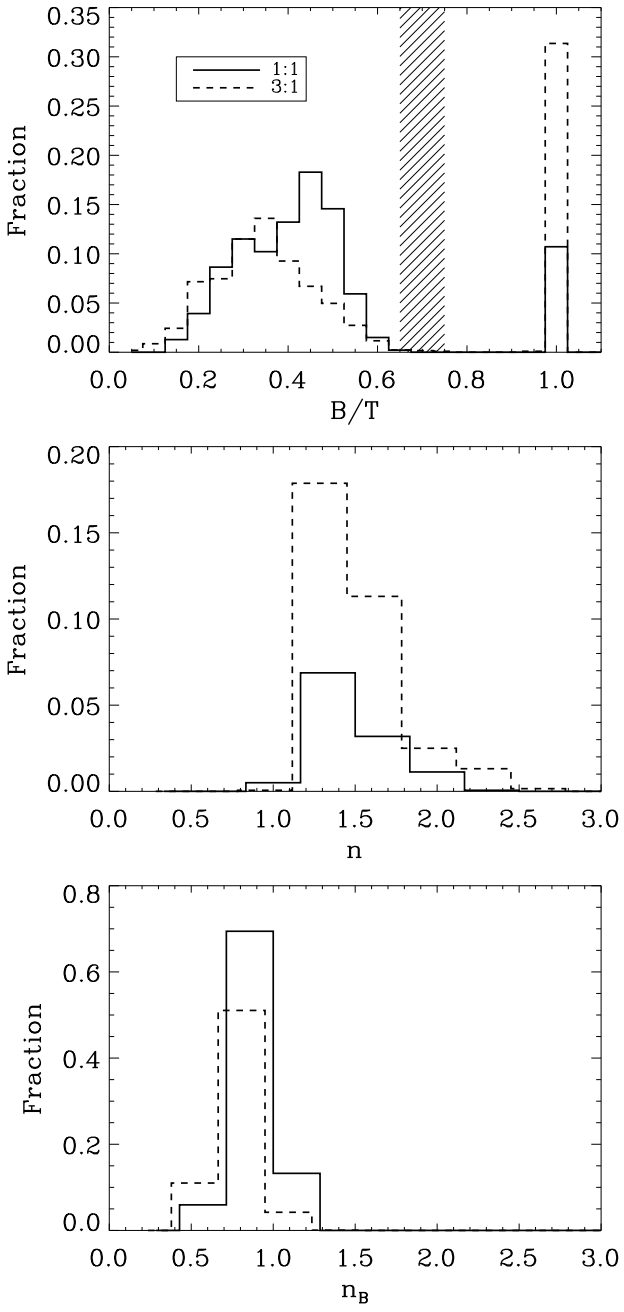

Figure 6. *Upper panel*: Histogram of the bulge–to–total ratio (B/T) for all projected 1:1 and 3:1 bulge-less merger remnants. The shaded area around $B/T = 0.7$ divides bulge + disc systems from pure bulge systems. *Middle panel*: Distribution of the Sérsic index for all projections classified as pure bulges for the projected 1:1 and 3:1 merger remnants without bulges. *Lower panel*: Distribution of the Sérsic index of the bulge components for the disc+bulge fits for the mass ratios 1:1 and 3:1.

ences in detail the results of González-García & Balcells (2005) and our results clearly indicate that collisionless merger remnants of pure disc systems do not evolve into concentrated systems with surface density profiles similar to giant elliptical galaxies. Mergers without bulges also have lower phase-space densities as we show for a typical

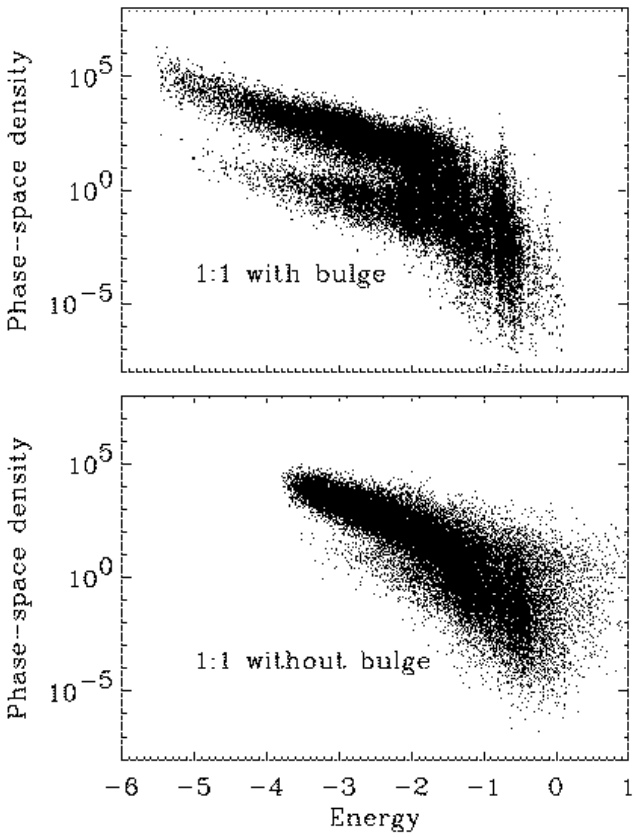

Figure 7. Phase-space densities for typical 1:1 merger remnant with and without a bulge in the progenitor disc. The merger without the bulge has a lower phase-space density.

example in Fig. 7. The remnant with bulge has more strongly bound particles and the maximum phase space density is at least a factor 10 larger than for the bulge-less remnant. The phase-space densities have been computed as in Ascasibar & Binney (2005) using the program kindly provided by the authors. This has been suggested for a long time (Ostriker 1980; Carlberg 1986; Hernquist 1993b) and has to be taken into account when interpreting simulations of stellar mergers of pure disc galaxies. In the following we only consider properties of remnants of mergers with bulges in the progenitor discs.

5 GLOBAL PARAMETER RELATIONS

In Figs. 8 and 9 we show the correlation between the disc scale length and the central surface density of the disc as well as the effective radius and the mean effective surface density of the bulge. In both cases there is a reasonably tight correlation in the sense that larger systems have lower surface densities. The bimodal distribution in Fig. 9 arises from the fact that there is no continuous transition between the systems classified as DB systems (upper left) and systems classified as one-component bulges (lower right). The trend for the correlations is surprisingly similar to observed galaxies (see e.g. de Jong et al. 2004; their Figs. 6 and 7). The correlation between the bulge effective radii and the disc scale lengths

is shown by the grey dots in Fig. 10. Systems with larger bulges also have larger discs. On average h_D is a factor of 3-5 larger than r_{eB}. In contrast, de Jong et al. (2004) (open squares in Fig. 10; here we have scaled the obervational data down by a factor 3 assuming an initial disk scale length of 3kpc for the model disc) find that bulges in observed early–type galaxies are on average only a factor of 2 smaller than the discs. This result might reflect the fixed B/T ratio in our initial conditions of our sample as we find a good agreement with observations for small bulge sizes. The few projections that are found to have similar sizes in both components also have the largest B/T values ($0.7 < B/T < 0.9$). As we have seen in Fig. 1 there are only a few projections in this regime.

In Fig. 11 we show, for every projection and all mass ratios, B/T versus the mean effective surface density, $< \Sigma_{eB} >$, the effective radius r_eB and the Sérsic index of the bulge component n_B. The points on the vertical line, $B/T = 1$, indicate the projected remnants classified as pure bulges. Observations from de Jong et al. (2004) are overplotted as open diamonds. There is a weak trend for galaxies with a larger B/T to have a smaller bulge effective surface density (upper panel of Fig. 11). In addition, galaxies with smaller B/T ratios also have bulges with smaller effective radii (middle panel of Fig. 11). There is a good general agreement with observations but still the bulk of the simulated projections have small bulge sizes. There is also a correlation between B/T and the Sérsic index of the bulge. Remnants with $n_B \approx 1$ have small values of $B/T \approx 0.3$ and n_B is increasing with increasieng B/T. A similar correlation has beeen found by de Jong et al. (2004) (open diamonds) for their large sample of observed early–type galaxies. However, the observed values for n_B have a larger spread and appear to be on average 20-30% larger for $B/T < 1$. The correlations for r_{eB} and n_B are much tighter for $B/T < 0.7$. In this regime they are also much tighter than the observed correlations (de Jong et al. 2004) which might be due to the fixed bulge-to-total ratio in the initial conditions. We found no other significant correlation of the profile properties with global properties of the remnants like anisotropy, isophotal shape, or shape of the line-of-sight velocity distribution. In particular, there is no correlation between the projected central velocity dispersion of the remnants (which varies from a mean value of $\sigma = 0.5$ for 6:1 remnants to a mean value of $\sigma = 0.68$ for 1:1 remnants in computational units) and the Sérsic index of the bulge. However, this correlation has been found to be rather tight for observed ellipticals (Graham et al. 2001; Vazdekis et al. 2004). As our simulations are scale free we can make the simple experiment and try to shift the velocity scale of the remnants to the region where the observed n shows a similar distribution peaked around $n = 3.5$. Using the Vazdekis et al. (2004) data this would correspond to a small velocity range of $130km/s \leqslant \sigma \leqslant 170km/s$. Galaxies with lower σ have smaller n, those with higher dispersion tend to have larger n. This would shift our more massive initial disc galaxy to the Milky Way regime. Taking the above considerations at face value we might conclude that only binary mergers of evolved early–type spiral galaxies with masses similar to the Milky Way contribute to the intermediate mass population of elliptical galaxies. Turning the argument around we can almost certainly exclude that the most massive ellipticals are made by binary mergers of disc galaxies. This is in agreement with the kinematical analysis of Naab & Burkert (2003).

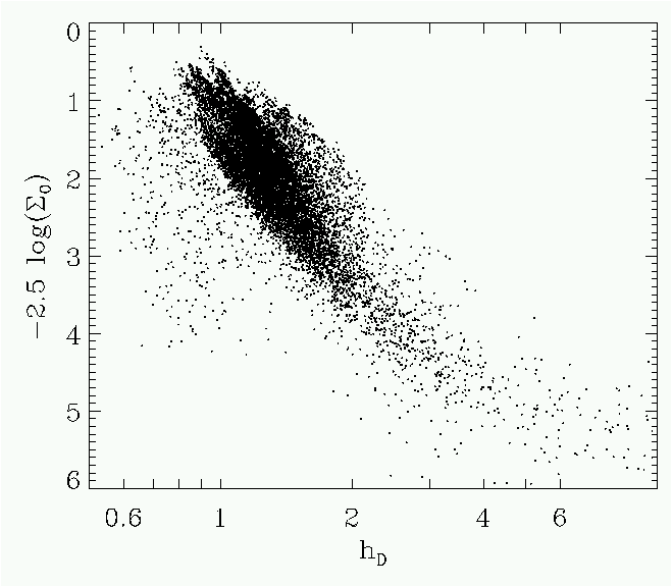

Figure 8. Disc scale length, h_D, versus the central surface density of the disc, Σ_0, for all remnants with bulges and all mass ratios.

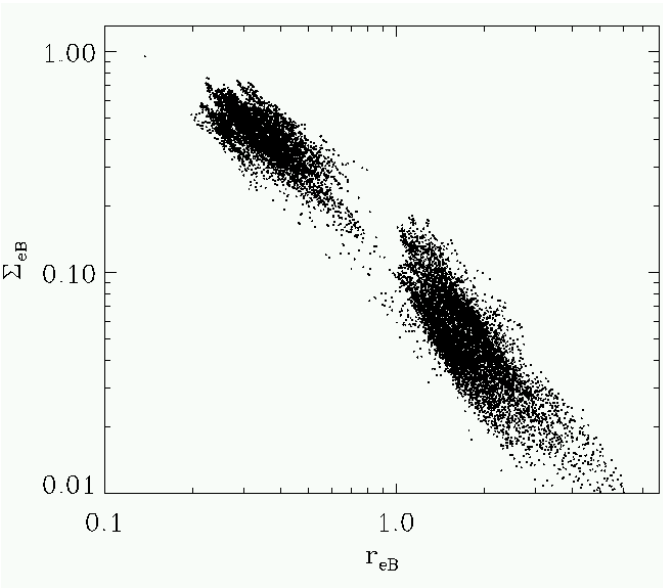

Figure 9. Effective radius of the bulge r_{eB} versus the mean effective surface density of the bulge, Σ_{eB}, for all projected remnants with bulges. If the galaxy was classified as a one component system we assumed $r_{eB} = r_e$.

6 IS THE EXPONENTIAL OUTER COMPONENT A REAL DISC?

In Fig. 12 we show the fraction of the 100 random projections of every remnant that were classified as a two-component systems (the rest was classified as one component systems) as a function of the initial geometry of the mergers. Only for a few cases, mostly for mass ratios 1:1 and

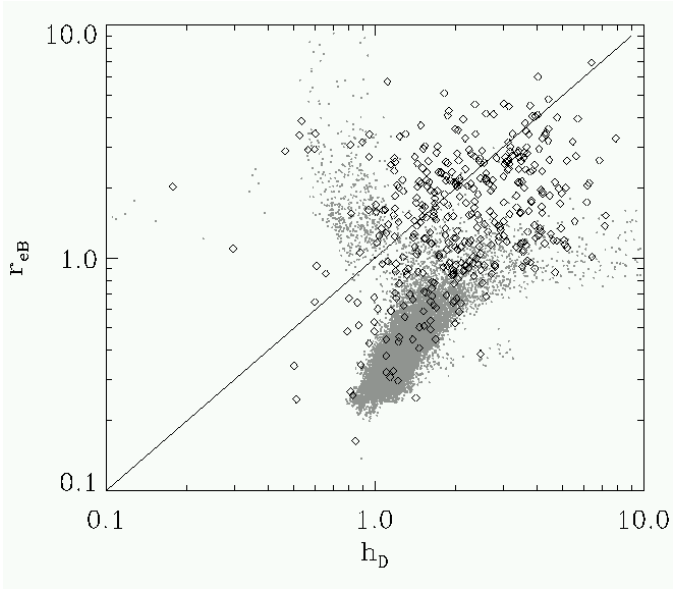

Figure 10. Disc scale length, h_D, versus the effective radius of the bulge, r_eB, for all projections (grey dots) assuming the best fitting disk+bulge model. Observational data for E/S0 galaxies from de Jong et al. (2004) are overplotted (open squares) and scaled down by a factor of 3 (same scaling as in Fig. 5) corresponding to an initial model disk scale length of 3kpc.

2:1, the remnant properties are independent of projection effects. Statistically we find a weak influence of the initial mass ratio or the initial geometry alone on the classification of the remnants. Typically the changes in classification are caused by a combination of different mass-ratios, initial geometries and projection effects. However, the presence of an outer exponential is a general feature which is common to most remnants. But what is the nature of this outer component? Naively one would assume that it represents a classical exponential disc. At least for 1:1 and 2:1 remnants this interpretation is questionable as e.g. Naab & Burkert (2003) have demonstrated that the kinematical properties of these remnants are very similar to slow-rotating hot stellar systems. Interestingly, if investigated in detail remnants of all mass ratios show similar degrees of anisotropy and the main kinematical difference appears to be the amount of rotational support (Binney 2005; Burkert & Naab 2005). On the other hand, the material in the outer regions of the remnants originates from the exponential disc component of the progenitor discs and the exponential profile of the remnants could point to this origin.

If the exponential component of the remnants was an outer disc it should be significantly flattened with a high ellipticity ($\epsilon \gtrsim 0.7$) if seen edge-on. Dynamically it should be significantly supported by rotation with the local ratio of the line-of-sight velocity and the velocity dispersion, v/σ, greater than unity. Proper discs in ellipticals might have significantly larger values than that (Rix et al. 1999), however there also exist S0 galaxies which have confirmed stellar disc components but $v/\sigma < 1$ (Rix et al. 1992; Rubin et al. 1992). In case of NGC 4550 this is caused by two counter-rotating discs which could only have been detected by detail kinematical analysis. In this sense the ellipticity might be the stronger constraint for our first order analysis.

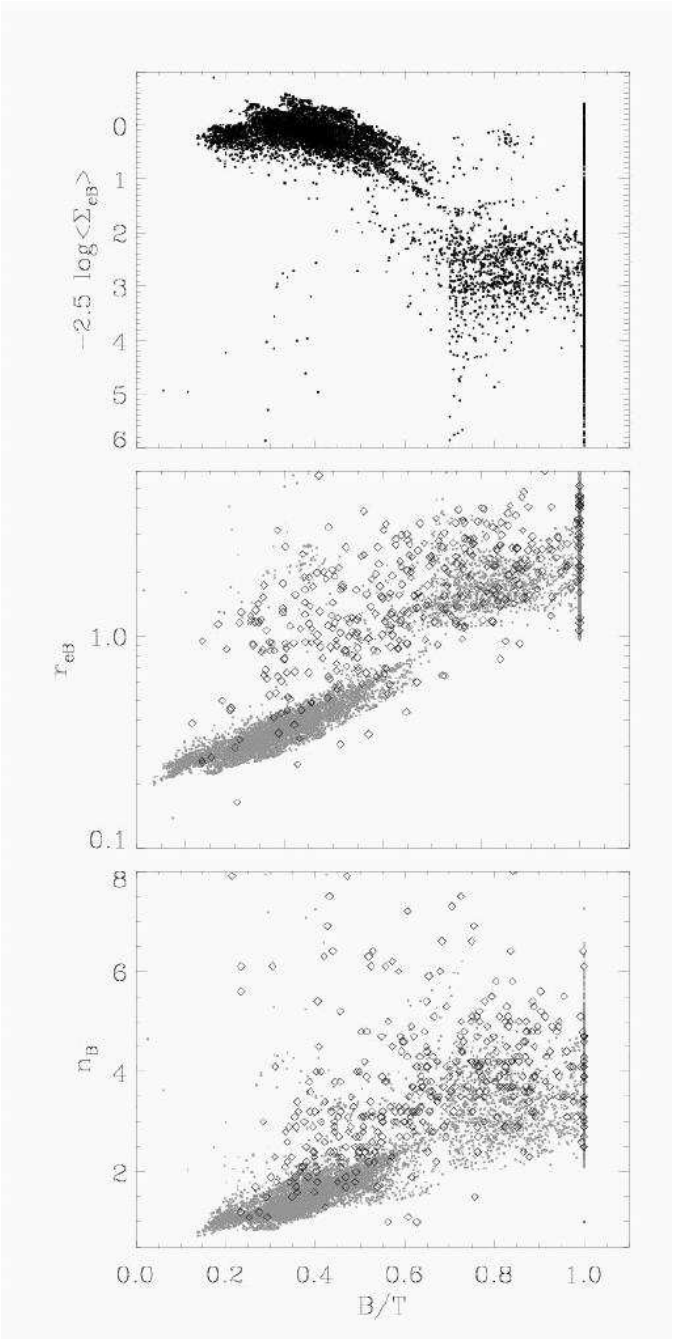

Figure 11. *Upper panel*: Mean effective surface density of the bulge versus B/T. *Middle panel*: Effective radius of the bulge versus B/T. For systems with $B/T = 1$ we use $r_{eB} = r_e$. *Lower panel*: Sérsic index of the bulge versus B/T. For systems with $B/T = 1$ we use $n_B = n$. We show all projected remnants with bulges in the initial condition discs. Observational data for E/S0 galaxies from de Jong et al. (2004) are overplotted (open squares) for the two lower panels and scaled down for r_{eB} by a factor of 3 (same scaling as in Fig. 5) which corresponds to an initial disk scale length of 3kpc.

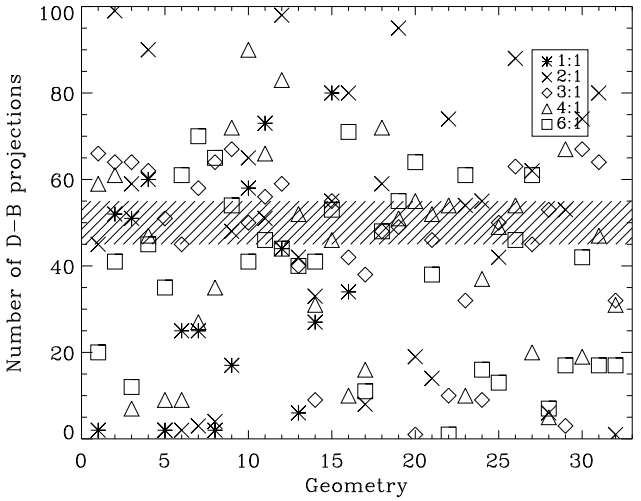

Figure 12. Number of projections (out of 100) classified as DB systems for mass ratios 1:1-6:1. The numbers on the abscissa indicate individual merger geometries with initial disc orientations as in Naab & Burkert (2003), Table 1.

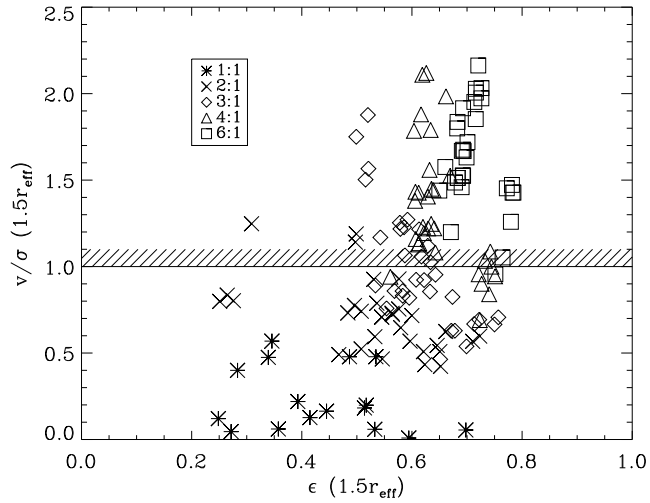

Figure 13. Local ratio of v/σ versus ϵ at $1.5r_e$ for the edge-on projections of all merger remnants. We assume disc-like properties if $\epsilon \gtrsim 0.65$ and $v/\sigma \gtrsim 1$.

To test the properties of the exponential components of the remnants we measure ϵ and v/σ at a radius of $1.5r_{eG}$ were the exponential component typically becomes dominant. Typical bulges in our remnants have sizes of $r_{eB} < 0.5r_{eG}$ (Fig. 4) and dominate only the center. In Fig. 13 we show the local values of $\epsilon_{1.5}$ and $v/\sigma_{1.5}$ at $1.5r_e$ for every remnant seen along the intermediate axis (edge-on). 1:1 and 2:1 remnants do not show high ellipticities and are dynamically hot. In this case the exponential outer component can not be associated with a disc. Its properties are more similar to hot outer halos of cD galaxies (Graham et al. 1996). Remnants with mass ratios of 6:1 on the other hand show very high ellipticities, $\epsilon_{1.5} \gtrsim 0.6$, and in general $v/\sigma_{1.5} > 1$, in some cases even $v/\sigma_{1.5} > 2$ which is a strong indication for the presence of an intact disc component that was heated during the merger. For comparison: the initial condition disc has $\epsilon_{1.5} = 0.85$ and $v/\sigma_{1.5} \approx 5$. 3:1 and 4:1 remnants have intermediate properties for which the two-component projections are in good agreement with the observed ellipticals with exponential outer profiles and elliptical-like kinematics as characterized by $v/\sigma \simeq 1$ (Jog & Chitre 2002). As proposed by Bekki (1998) 6:1 and 4:1 remnants are good candidates for S0 galaxies (see also Bournaud et al. 2004). They show strong evidence for a heated disc component but still elliptical like surface density properties in some projections indicating that depending on the projection the remnants would be classified as S0 or elliptical galaxies. We do not find outer components with a flattening smaller than $\epsilon = 0.2$ which is probably due to the limited heating during the interaction process. Note that only the strongly interacting mergers with mass ratios of 1:1 and 2:1 lead to values of $\epsilon < 0.45$

Bournaud et al. (2004, 2005) have analysed disc merger simulations including star formation and argue that ellipticals with outer exponentials can be produced by mergers with mass-ratios in the range 4.5:1 to 7:1. Based on our larger statistical sample (however, without star formation) we conclude that all mass ratios can lead to remnants with outer exponential profiles and elliptical-like kinematics. We can think of several possible reasons for the subtle differences in the conclusions: either the presence of a dissipative component and star formation changes the properties of mergers with mass ratios of 1:1 to 3:1 or Bournaud et al. (2005) have missed the exponential components due to their simple classification criterion. In addition, Bournaud et al. (2005) use different initial conditions and a different numerical algorithm (grid code) with a spatial resolution that is a factor of two lower than for our simulations. Taking all these differences into account the general behaviour of remnants with mass ratios larger than 3:1 is in good agreement.

The orbital structure of the remnants provides additional evidence that the structure of the exponential outer components change with mass ratio. Jesseit et al. (2005) have shown that at radii larger than the effective radius 1:1 remnants have equal amounts of box (box+boxlet) and tube orbits. In some cases major-axis tubes are also populated to a similar degree as minor-axis tubes supporting a round shape. On the other hand, 3:1 and 4:1 remnants are, at larger radii, clearly dominated by tube orbits. Tube orbits carry the angular momentum in the systems and are the typical orbits in stellar discs.

7 SUMMARY & DISCUSSION

The surface density profiles of an unbiased sample of simulated stellar merger remnants of disc galaxies with bulges (mass ratios 1:1, 2:1, 3:1, 4:1, and 6:1) and without bulges (mass ratios 1:1 and 3:1) in the progenitor discs have been investigated in detail. Every remnant has been analysed from 100 random viewing angles resulting in 19200 projected remnants in total. We have fitted the profiles using a single Sérsic function, and a Sérsic function plus an exponential. Based on the resulting bulge–to–total ratios — systems with high

bulge–to–total ratios ($B/T > 0.7$) were considered as one component — and the quality of the fits we have classified the projected remnants either as one- or two-component systems. In general the classification of every remnant changes with its projection and we find no strong correlation between the surface density properties of the remnants and the mass ratio of the initial discs.

Collisionless mergers of pure disc systems do not result in compact remnants similar to elliptical galaxies with large central phase space densities. Most simulated remnants show a two-component structure with Sérsic indices of the bulge $n_B < 1$. In those cases where the profile is well fitted with a single Sérsic function the profiles are inconsistent with $n > 2$ and therefore inconsistent with properties of observed giant elliptical galaxies confirming earlier results (Ostriker 1980; Carlberg 1986; Hernquist 1992). An additional gas component in the progenitor discs might be able to solve this problem. It does, however, lead to a concentrated peak of stars at the center unless very efficient feedback processes are included (Mihos & Hernquist 1996; Springel et al. 2005; Cox et al. 2005). Interestingly, some observed nearby merger remnants do show exponential K-band profiles (Rothberg & Joseph 2004) which would indicate that their progenitors did not have concentrated bulges. Whether those observed remnants will evolve into bonafide ellipticals will depend on the amount of available gas and when and where it is transformed into stars. Recently, Robertson et al. (2005) showed that gas in disc mergers can change the central velocity dispersionsof the remnants and can contribute significantly to the tilt of a the Fundamental Plane made by merger remnants. A full analysis of the surface density properties is, however, still missing.

Merger remnants of discs with bulges cover a wide range of bulge–to–total ratios ($0.2 < B/T < 1$). At every mass-ratio more than 50% of the projected remnants can be considered as one-component systems with a very similar Sérsic index distributions in the range of $2 < n < 6$. For all mass ratios the distributions peak in the range $3 < n < 4$. Statistically the photometric sizes of the remnants are of the same order than the size of the initial disc, independent of the mass ratio. In some projections the remnants can appear 50-100% larger, in other projections the remnants can even appear smaller than the initial disc. Surprisingly, the difference in kinematic properties for different mass-ratios (Naab & Burkert 2003) is more significant than the difference in the properties of the surface density profiles. We do not find correlations between the surface density profiles of our remnants and global properties like velocity dispersion or isophotal shape. As our models are scale free we can not explain the observed correlations between luminosity or velocity dispersion and shape index of the whole population of elliptical galaxies with our models alone. However, if our initial discs were scaled to a Milky Way-type galaxy the properties of the remnants would be consistent with intermediate mass early–type galaxies in the range of $-20 < M_B < -18$. This further supports the scenario that only part of the present day elliptical galaxy population can have formed by binary mergers of discs (Naab & Burkert 2003). More massive ellipticals are likely to have formed by a different process, e.g.early (Naab et al. 2005) or late multiple mergers (Weil & Hernquist 1996) and/or mergers of early type galaxies (e.g. Bell et al. 2005; González-García & van Albada 2005; Naab et al. 2006, and references therein). Of course the above conclusion is limited to our choice of initial conditions. Allowing for varying bulge-to-disc ratios and sizes for the initial discs with consistent bulge profiles might lead to remnants that follow the observed correlations. A first step in this direction has been attempted by Aceves & Velázquez (2005). They did, however, not include bulge components in their initial discs which is problematic (see above) and a consistent study is therefore still missing. Furthermore we have been investigating the limiting case that the progenitor galaxies are gas free. It is not clear in how far the presence of gas and the uncertain physics of star formation and feedback will influence the surface density properties statistically. We can expect stronger changes for discs with higher gas fractions. Another study that has to be done in the future.

More than 40% of all remnants at all mass-ratios show clear signatures of an outer exponential component. We have used additional local kinematic and photometric information at $1.5r_{eff}$ to determine the nature of this exponential component which is not possible by photometry alone. We found that the properties of the exponential component changes with mass ratio: For 1:1 and 2:1 remnants it resembles a dynamically hot spheroidal halo and for 6:1 remnants it resembles a flattened disc supported by rotation. 3:1 and 4:1 remnants have intermediate properties. It is known that the violent process during 1:1 and 2:1 mergers destroys the initial disc structure while higher mass ratio mergers are less violent and tend to preserve the discs of the more massive progenitor (Naab & Burkert 2003; González-García & Balcells 2005; Bournaud et al. 2005). This interpretation is supported by the fact that 3:1 and 4:1 remnants are significantly more dominated by tube orbits in their outer parts than 1:1 remnants (Jesseit et al. 2005). We have shown that even collisionless 1:1 remnants, despite the violent merging, remember their initial state to some extend and can keep their outer exponential particle distribution. Observationally, de Jong et al. (2004) find that most early-type galaxies show an exponential outer component if a two component fit is performed. The physical meaning of this finding is, however, still uncertain. We conclude that exponential outer components are a generic feature of binary disc mergers. They might directly indicate that mergers involving exponential stellar discs have played an important role during the formation of early-type galaxies. Of course there are other possibilities for the origin of outer exponential components. They might have formed from left-over gas after a disc merger (Naab & Burkert 2001a; Barnes 2002; Springel & Hernquist 2005), accretion of small satellites, accretion of gas from the halo followed by star formation etc. As all our 1:1-4:1 remnants have kinematic properties that are comparable to elliptical galaxies (Naab & Burkert 2003) we can naturally explain observations of galaxies with elliptical-like kinematics but exponential-like profiles (Jog & Chitre 2002). In agreement with Bournaud et al. (2004) we find that the effect is strongest for high mass-ratios. In contrast to Bournaud et al. (2004) we find that those systems can also form from mass ratios 1:1 - 4:1 and we do not see a sharp transition when changing the mass ratio from 4:1 to 6:1.

We have found distinct correlations between the parameters from the surface density fits: (1) the sizes of the exponential component and the bulge are correlated; (2) a sys-

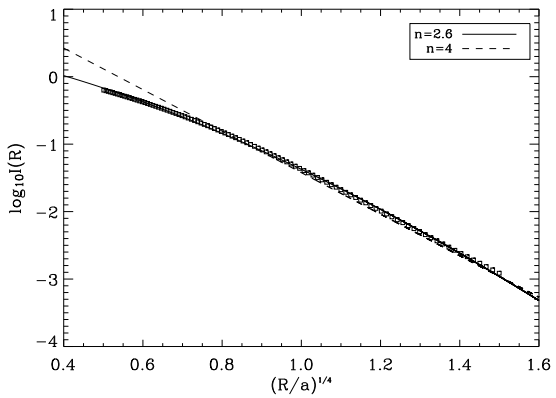

Figure A4. Projected Hernquist (1990) density profile with scale length a (open boxes). The best fitting Sérsic fit (solid line) has $n = 2.6$ as the projection deviates significantly from a de Vaucouleurs (1948) profile with $n = 4$ (dashed line) at radii $(r/a)^{1/4} < 0.8$.

tem with a larger bulge-to-total ratio has on average a larger Sérsic index, a larger bulge effective radius and a lower effective surface density; (3) larger bulges have a lower effective surface density. These results are in good agreement with observations of early–type galaxies (see e.g. de Jong et al. 2004).

If compared to nearby merger remnants the range and distribution of Sérsic indices of the remnants are comparable to the observations (Rothberg & Joseph 2004). In particular, nearby remnants – similar to simulated remnants – do not show correlations between the surface brightness profiles and other global properties like velocity dispersion or isophotal shape. We can therefore conclude that disc galaxies are the likely progenitors of the observed remnants. They probably evolve into elliptical galaxies in the future. The time-scale for this process, however, depends on the stellar populations of the remnants and can in principle be assessed applying evolutionary models for disc galaxies (e.g. Naab & Ostriker 2006) to N-body models.

ACKNOWLEDGMENTS

The authors thank Yago Ascasibar for kindly providing his software to compute the phase-space densities. We also thank John Kormendy, Ralf Bender, Roberto Saglia, Alister Graham, Fabian Heitsch and Roland Jesseit for interestings discussions and valuable comments on the manuscript and Roelof de Jong and Barry Rothberg for kindly providing their observational data. Finally we thank the referee Reynier Peletier for his valuable comments which improved the manuscript.

APPENDIX A: INDIVIDUAL EXAMPLES

To demonstrate the quality and the limitations of the surface density analysis we show and discuss the surface density fits of the initial condition disc and disc+bulge model as well as of one merger remnant of every mass ratio, respectively.

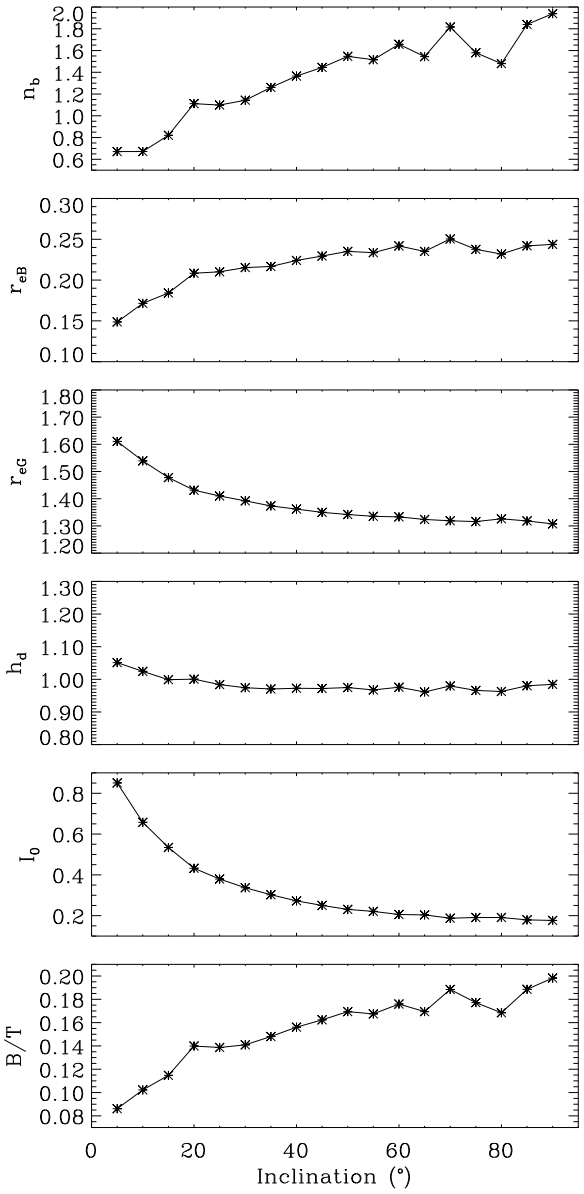

Figure A5. Variation of the fitting parameters for the initial condition disc+bulge system with inclination angle (0^o is edge-on, 90^o is face-on). The Sérsic index of the bulge, n_B, the size of the bulge, r_{eB}, and B/T increase from edge-on to face-on, the global size, r_{eG}, decreases due to an apparently more dominant bulge component. The disc scale length h_d does not change with inclination. The central surface density I_0 of the disc is highest for the edge-on case and decreases strongly towards face-on.

A1 Initial conditions

Fig. A1 shows the real isophotes and the best fitting ellipses, the surface density analysis and the residuals for the initial condition disc-only model as seen tilted by 5^o, 45^o and face-on. The parameters for the Sérsic–only and the bulge+disc fits are given in the middle panel. All three projections of the system are classified as one component systems with close to exponential density profiles. The analysis program was able to recover the initial condition parameters almost perfectly if the disc is seen face-on (last row in Fig. A1). If the galaxy

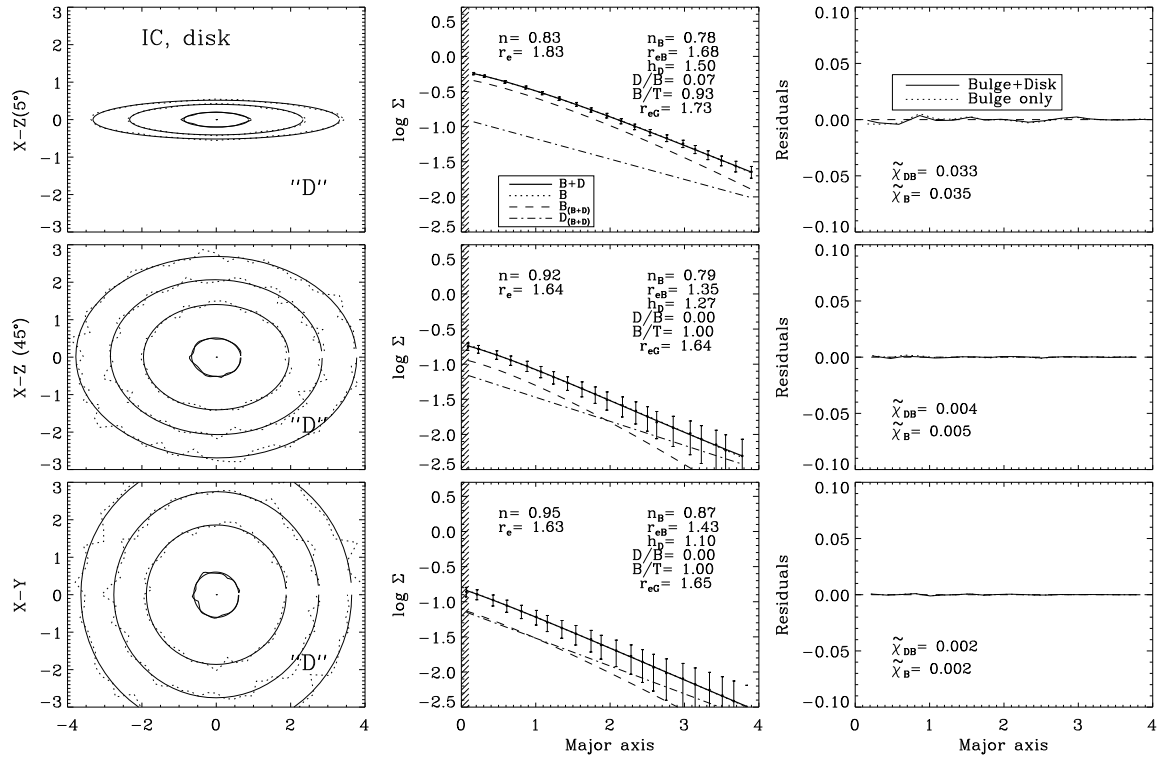

Figure A1. Surface density analysis for the initial disc as used for the bulge-less mergers. *Left panel*: Contours of the projected surface density (dotted) with fitted ellipses (solid) inclined by 5^o (upper plot), 45^o (middle plot), and seen face-on (lower plot). *Middle panel*: Surface density profiles along the major axis of the respective projection (dots with error bars). The best fitting DB-model is shown by the thick solid line. The disc and bulge contribution is indicated by the thin dot-dashed and the dashed line, respectively. The thick dotted line shows the best fitting Sérsic-only model, which is in this case close to an exponential. The shaded area indicates the radial range influenced by the force softening and has been excluded from the fitted data points. *Right panel*: Residuals for the two fits and the corresponding reduced chi–squared values. This is a one component system with an exponential surface density profile and for the face-on projection we can recover the input parameters. For $n = 1$ the disc scale length h_D is related to the effective radius like $r_e = 1.676 h_D$. Observed in projection towards edge-on the shape parameter decreases and the size increases by 10%.

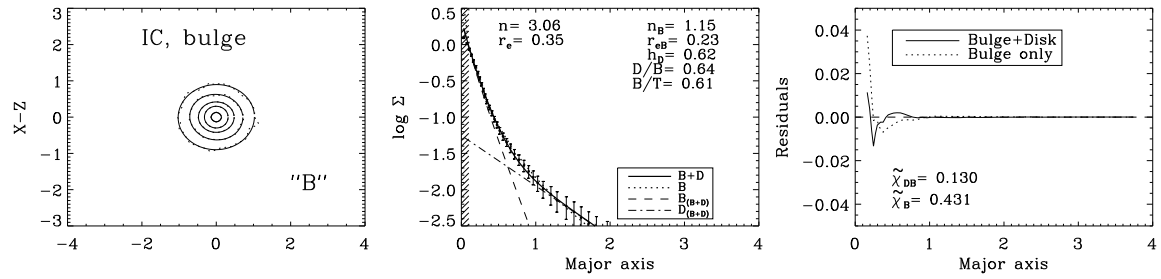

Figure A2. Surface density analysis as in Fig. A1 but for the initial bulge system only. Note that the projected Hernquist-bulge does not perfectly follow an $r^{1/4}$ profile. The theoretically expected value for the effective radius, $r_e = 0.36$, is similar to the fitted value. The BD-fit does not improve the quality of the fit in this case as the reduced chi–squared for the Sérsic-only fit is already well below unity.

is seen more edge-on the shape parameter decreases and the size increases by more than 10%. Note that for a Sérsic–profile with $n = 1$ (exponential profile) the scale length h_D is related to the projected effective radius like $r_e = 1.676 h_D$.

In Fig. A2 we show the analysis for the bulge component separately. The scale length a_H of the Hernquist-spheroid is related to its effective radius, r_{eH}, as $r_{eH} = a_H(1 + \sqrt{a_H})/1.33$. For the model used here with a scale length of $a_H = a_b = 0.2$ this would result in $r_{eH} = r_{eB} = 0.36$. This value can be recovered by the fit. We note here that the projected Hernquist density distribution follows a de Vaucouleurs like $r^{1/4}$ profile only at radii larger than half its scale length. If analysed over the full radial range the best fitting Sérsic-index for the projected Hernquist (1990) density distribution would be $n = 2.6$ (see Fig. A4) which is lower than the value of our bulge, $n = 3.06$, (see Fig. A2) as we exclude the more flattened innermost parts from the fit.

The analysis for the composite disc+bulge model is shown in Fig. A3. The fitted scale length of the disc seems in good agreement with the initial parameters (Section 2),

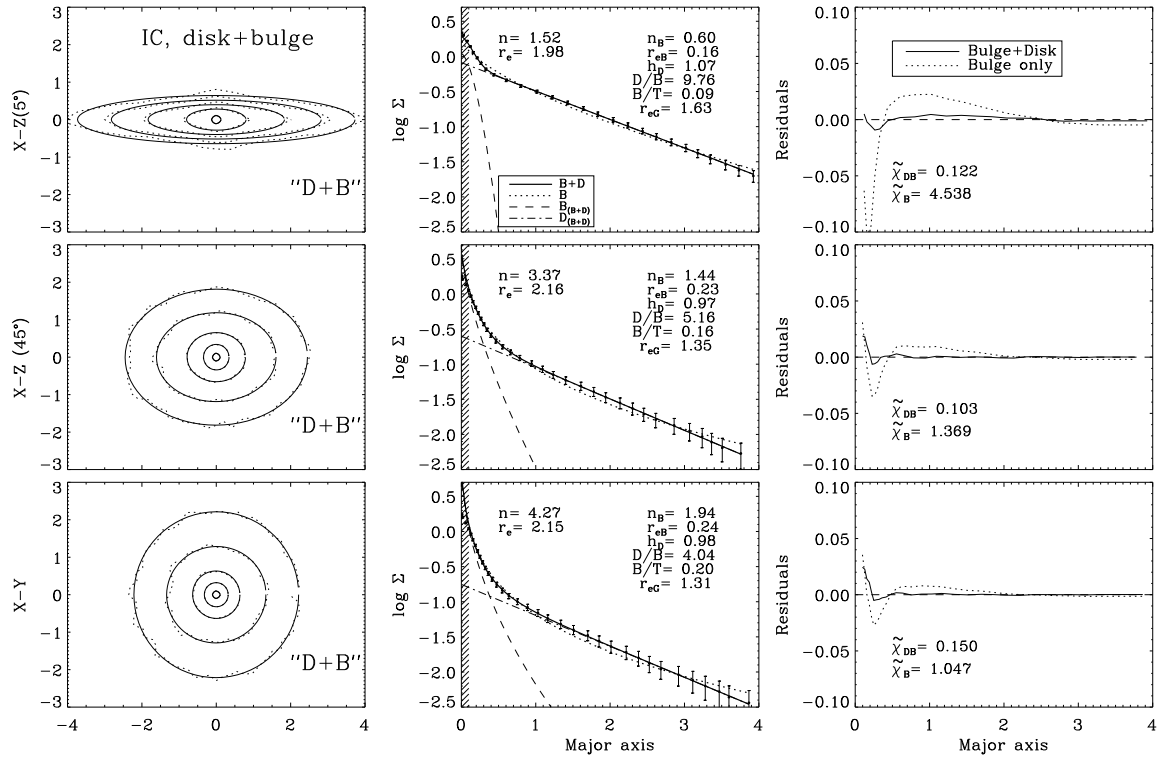

Figure A3. Surface density analysis as in Fig. A3 but for the initial disc+bulge model. For the face-on projection we can nearly recover the input parameters. However, the size, mass fraction and curvature of the bulge is underestimated if compared to the two individual components (see Figs. A1 and A2). The effect get stronger if the galaxy is seen more edge-on.

independent of projection. The best agreement with the theoretically expected values is achieved for the face-on projection. The disc–to–bulge ratio $D/B = 4.04$ is 25% larger than the dynamical input value of $M_d/M_b = 3$. The shape parameter of the bulge, $n_B = 1.94$, is smaller than for the isolated bulge. The maximum projected size of the bulge is equal to the isolated bulge model. If projected nearly edge-on the bulge–to–total ratio drops below $B/T = 0.1$ and the system appears to be disc dominated except from the very inner parts. The apparent size and Sérsic-index of the bulge in the edge-on projection are significantly smaller. Part of the outer bulge material is counted as disc material to guarantee an exponential projected profile – which does not represent the intrinsic disc distribution for this projection (see Fig. A1). The bulge can then very well be fitted with an exponential as only the inner part of the bulge is accessible. In Fig. A5 we show how the fitting parameters change with disc inclination. The shape index of the bulge changes almost linearly from $n_B \approx 0.6$ in the edge-on projection to $n_B \approx 2$ in the face-on projection. The bulge is also smaller if seen edge-on. The system as a whole appears larger in the edge-on projection. The global effective radius of the initial bulge+disc system has been calculated using Eqn. 6 and is in the range of $1.3 < r_{eG} < 1.6$. The values are lower than for the pure disc system (Fig. A1) due to the additional centrally concentrated bulge component. The disc scale length, h_d, does not change with projection, in contrast to the disc only model (Fig. A1). The central surface density of the disc, however, changes strongly with inclination, especially at inclinations smaller than 40^o (towards edge-on). This effect has already been investigated with a simple model (see e.g. Graham 2001). The bulge-to-total ratio is in the range of $0.09 < B/T < 0.2$ and is increasing from edge-on to face-on. The increase is strongly correlated with the increase of n_B. These results indicate that observed disc–to–bulge ratios of early-type disk galaxies might be systematically overestimated and Sérsic-indices of bulges might be systematically underestimated if the galaxies are inclined with respect to the face-on projection. This effect might be partly responsible for part of the scatter in the observed $B/T - n$ relation (Andredakis et al. 1995) and we propose to investigate projection effects of observed disc galaxies in more detail. It also seems difficult to reconstruct the underlying mass distribution of the disc and the bulge as the low density part of the bulge is masked by the disc. In this way 20% - 35% of the bulge material (depending on the projection) could remain undetected in observed disc galaxies. The above results are stable and do not change significantly if we vary the fitting parameters like weights, inner boundaries, starting values etc. However, the details might depend very well on our choice of the initial conditions. The Hernquist spheroid is a good but not the optimal model for real bulges and more sophisticated bulge models that reproduce the observed properties might be useful for further investigations.

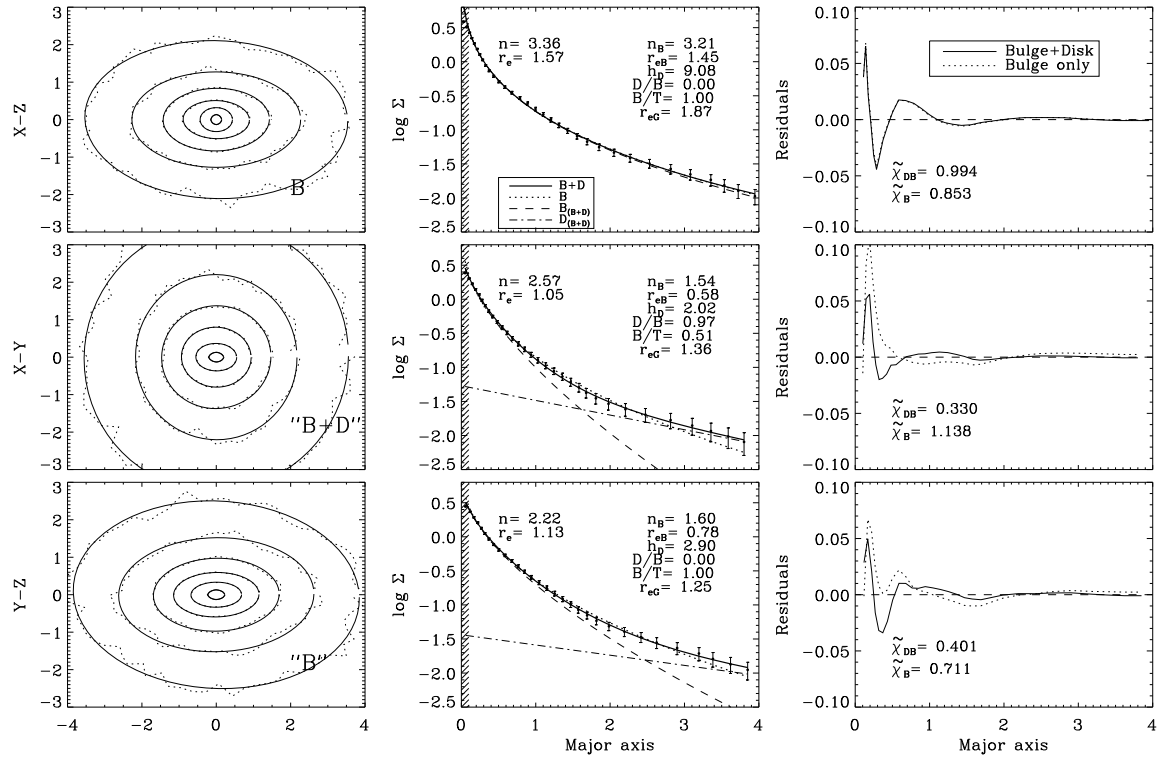

Figure A6. Surface density analysis as in Fig. A3 but for a 1:1 merger remnant projected along its three principal axes. Based on the selection criteria described in Section 3 the remnant would be classified as a pure bulge system in the first and third projections and as a bulge+disc system in the second projection.

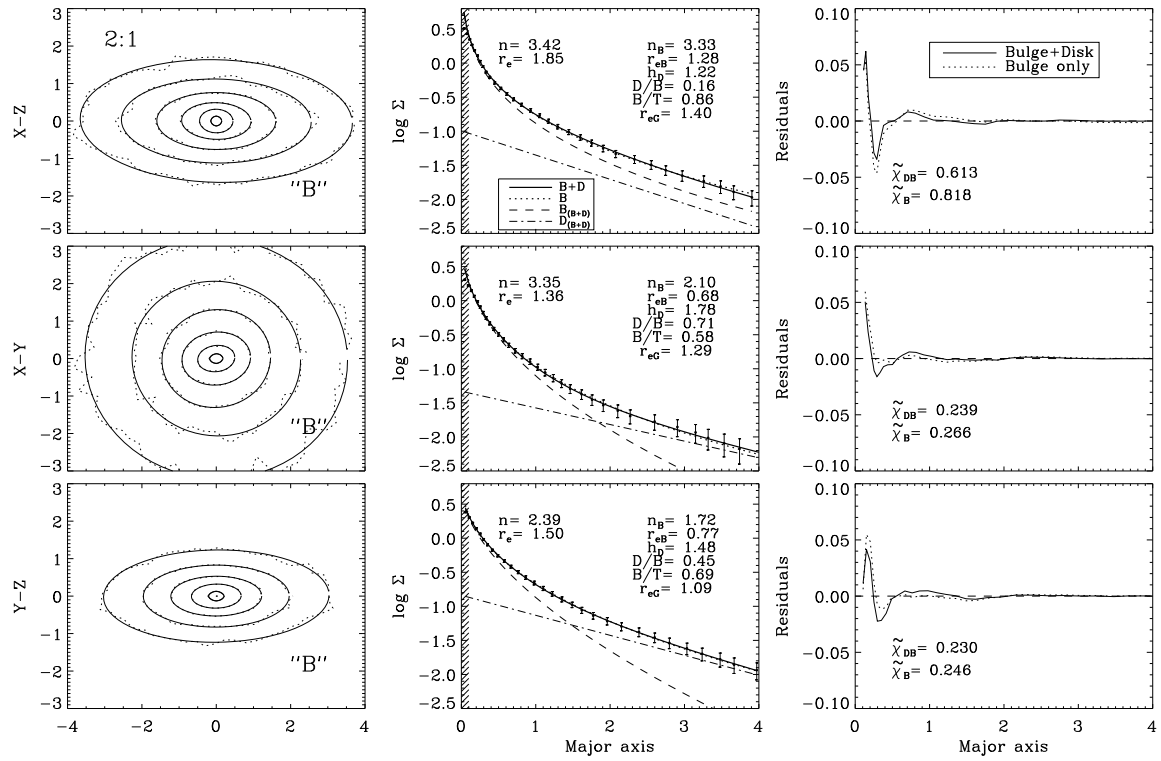

Figure A7. Same as Fig. A6 but for a 2:1 remnant. If observed, the remnant would be classified as a bulge in all three projections.

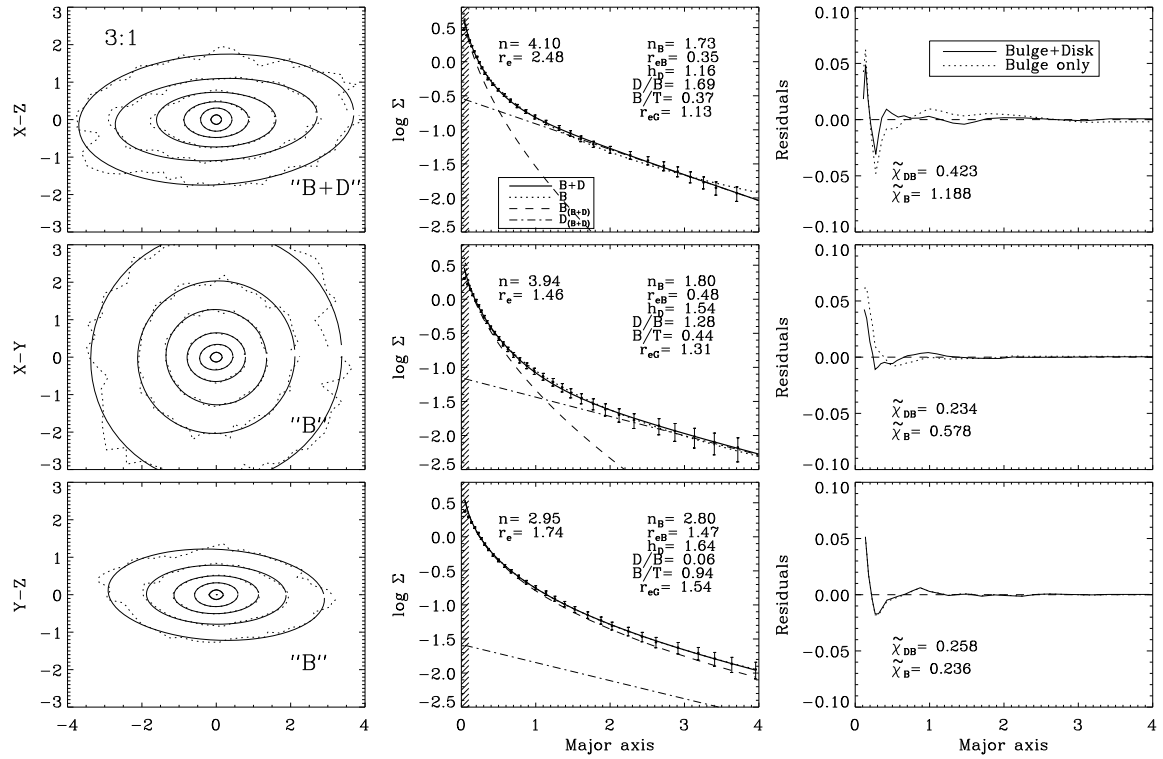

Figure A8. Same as Fig. A6 but for a 3:1 remnant. If observed, the remnant would be classified as a disk+bulge system in the projection along the intermediate axis (first row) and as a pure bulge system in the other two projections.

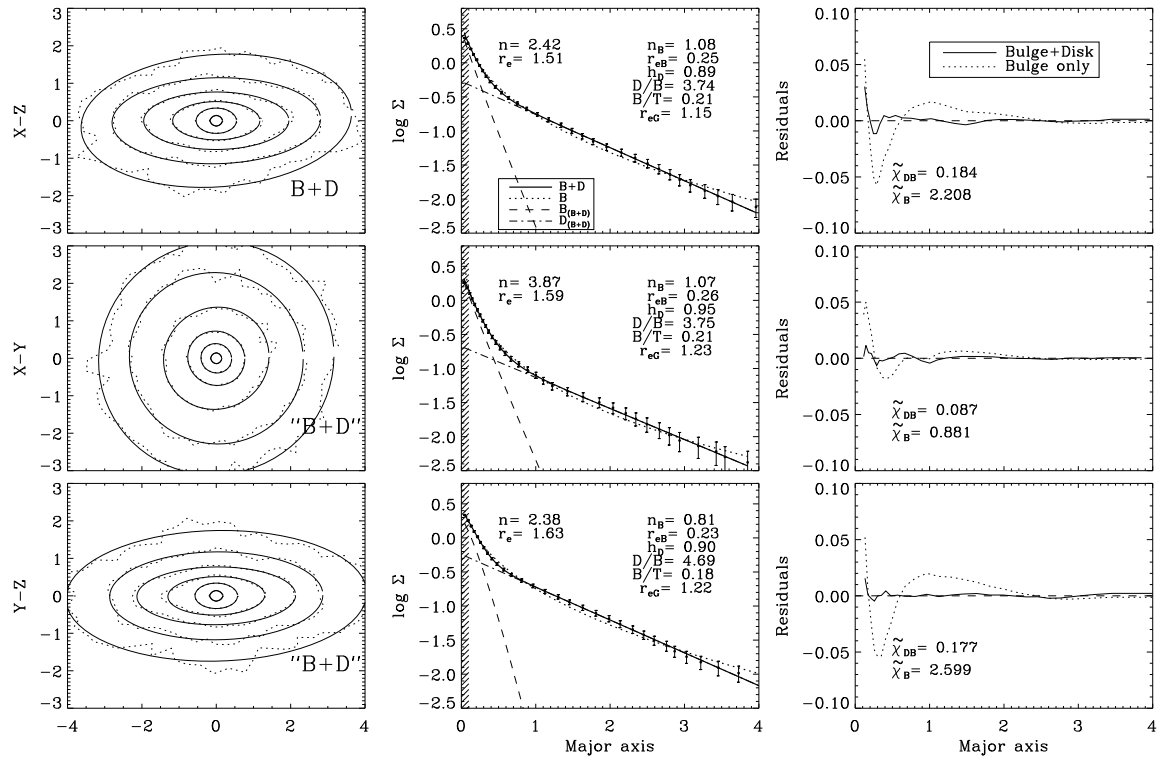

Figure A9. Same as Fig. A6 but for a 4:1 remnant. If observed, the remnant would be classified as a disc+bulge system in all three projections.

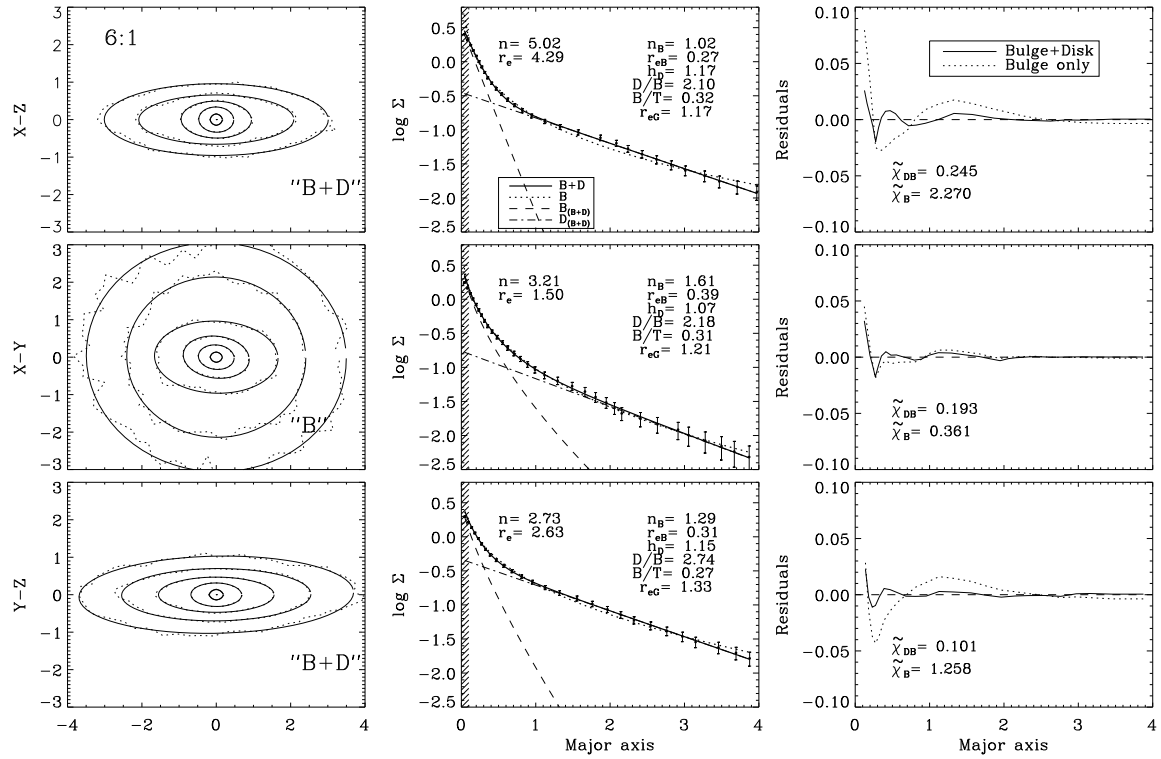

Figure A10. Same as Fig. A6 but for a 6:1 remnant. If observed, the remnant would be classified as a disc+bulge system in the two edge-on projections.

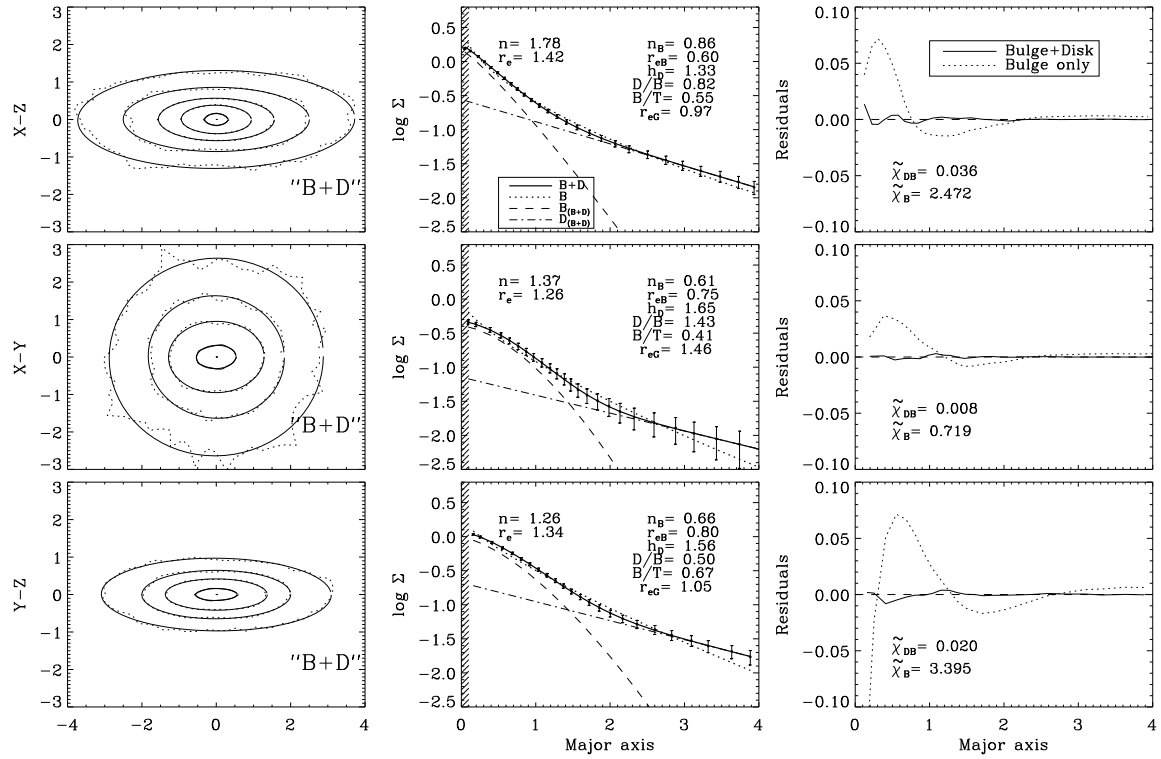

Figure A11. Same as Fig. A6 but for a 1:1 remnant without a bulge in the progenitor disc. If observed, the remnant would be classified as a disc+bulge system in all projections. The system is significantly less concentrated than the 1:1 remnant with bulge (Fig. A6).

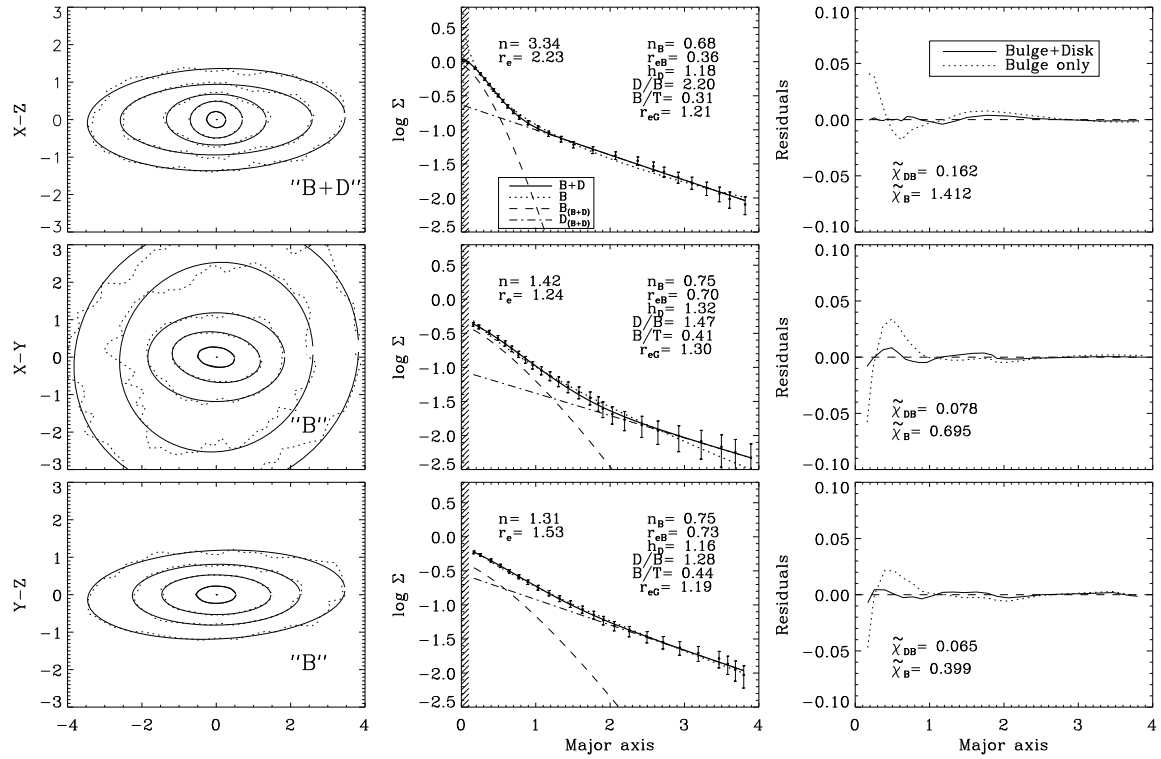

Figure A12. Same as Fig. A6 but for a bulge-less 3:1 remnant. If observed, the remnant would be classified as a disc+bulge in the first and as a bulge in the second and third projection. The remnant is prolate at the center and appears more concentrated if seen along the prolate structure (first row).

A2 Individual merger remnants

In Figs. A6 to A10 we show individual examples of the surface density analysis of disc+bulge merger remnants with mass ratios of 1:1, 2:1, 3:1, 4:1, and 6:1, respectively. A 1:1 and 3:1 remnant of mergers of two pure disc galaxies are shown in Figs. A11 and A12. All remnants are projected along the three principal axes of their moment-of-inertia tensor calculated form the 40% most tightly bound particles. The first projection in Fig. A6 represents a typical system that is classified as a one component bulge system. The freedom of adding an exponential component does not increase the quality of the fit. The second projection is classified as a disc+bulge system based on its bulge–to–total ratio and the better quality of the fit. The third projection would be classified as a one-component bulge system as the reduced chi–squared of the fit is below unity and $P < 0.32$ (Eqn. 7). To test for the effect of resolution we have re-simulated this remnant with a factor of 2 and 4 more particles and did not find a change in the properties exceeding the errors of the fitting parameters (Section A3).

All three projections of the 2:1 remnant shown in Fig. A7 can be fitted by a pure bulge model with sufficient accuracy. The first projection of the 3:1 remnant in Fig. A8 is classified as a disc+bulge system whereas the other two projections appear to be pure bulge systems. An example for a system with strong indications for an outer exponential component is the 4:1 merger remnant shown in Fig. A9. The first and third projections ("edge-on") clearly show two component systems. For the face-on projection both fits would result in a reduced chi–squared below one. However, only for the DB fit $P < 0.32$ and the system is classified as a BD system. The 6:1 remnants shown in Fig. A10 shows prominent exponential components in the "edge-on" projections. However, if seen face-on it would still be classified as a single bulge. Fig. A11 shows the surface density profile of a bulge-less 1:1 merger remnant. Due to the absence of the bulge the profile is significantly flatter at small radii than the corresponding remnant with bulge (Fig. A6). In all the projections the remnant does not have the characteristics of a single component system. The inner component is better represented by Sérsic function with a shape parameter $n_B < 1$, even close to a Gaussian with $n = 0.5$. A 3:1 remnant without bulge is shown in Fig. A12. In the first projection the remnant is classified as a two component system with a very shallow inner component. The two remaining projections appear like one component systems, however, with shape indices $n < 2$. This remnant has very prolate structure at the center which is typical for remnants without bulges. They appear more concentrated if projected along this structure (first rows in Fig. A11 and Fig.A12).

Already this first analysis clarifies that different projections of one merger remnant can lead to different fitting parameters. The ranges covered in B/T and Sérsic-indices are large and, in most cases, the classification of the merger remnant changes depending on the projection. It is therefore not possible to make any reliable statement based on individual projections of merger remnants and only a statistical analysis, as presented in Section 4, of the whole homoge-

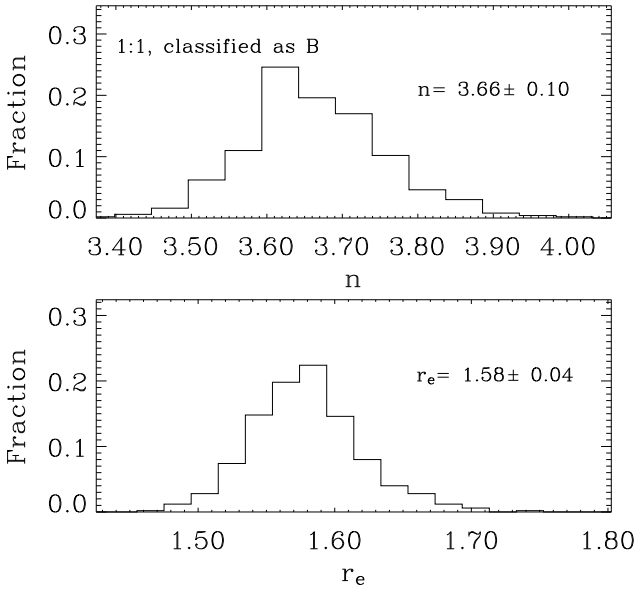

Figure A13. Typical distribution of the Sérsic-index (upper panel) and the effective radius (lower panel) for a fixed projection of a 1:1 merger remnant classified as a bulge for 500 independent realizations using the boots-trapping method. The distributions are narrow and the errors are well below 5%.

nous sample of simulations will allow us to draw any global conclusions.

A3 Stability of the analysis

We used the boots-trapping method (Heyl et al. 1994; Naab & Burkert 2003) to estimate the typical errors of the derived fit parameters. For this analysis we created 500 resampled realizations of one projection of the original N-particle distribution by selecting N particles from the remnant with replacement. For every realization some particles might appear several times and some might not appear at all. Thereafter we performed a full surface density analysis for all 500 realizations and computed the mean values and the standard deviations of the resulting fit parameters. We have selected two typical merger remnants as test cases: a projected 1:1 remnant that was classified as a were described primarily by the exponential component. To avoid these cases, the algorithm checks whether the central intensity of the fitted exponential component is larger than the central intensity of the fitted Sérsic bulge system and a projected 3:1 remnant classified as a disc+bulge system.

Fig. A13 shows the distribution of values for the Sérsic-index and the effective radius for the 1:1 test case which was classified as a bulge. In both cases the distribution is very narrow and the error is below 5%. The distribution for the four fitted values — Sérsic-index of the bulge, effective radius of the bulge, scale length of the disc and bulge–to–total ratio — of the 3:1 remnant classified as DB is shown in Fig. A14. The errors are larger than for the 1:1 remnants but still only of the order of 10%. The most important result of this analysis is that the variation in properties for different projections as shown in the previous section is real and not dominated by errors. The errors given here are typical and can be used for all following plots.

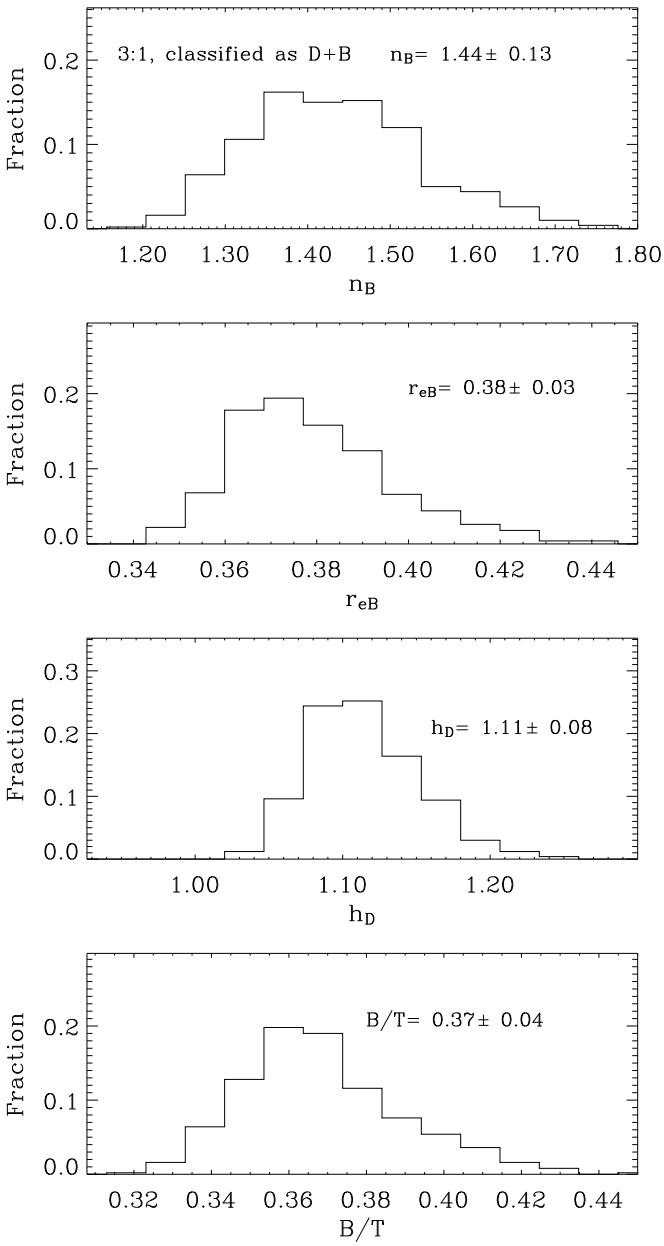

Figure A14. Boots-trapping analysis for 500 independent realizations (as in Fig. A13) of a typical 3:1 merger remnant classified as a disc+bulge system seen from a fixed projection. The errors for the Sérsic-index of the bulge, the effective radius of the bulge, the disc scale length and the bulge–to–total ratio do not exceed the 10% level.

REFERENCES

Aceves H., Velázquez H., 2005, MNRAS, 360, L50
Aguerri J. A. L., Trujillo I., 2002, MNRAS, 333, 633
Andredakis Y. C., Peletier R. F., Balcells M., 1995, MNRAS, 275, 874
Ascasibar Y., Binney J., 2005, MNRAS, 356, 872
Barnes J. E., 1992, ApJ, 393, 484
Barnes J. E., 1998, in Saas-Fee Advanced Course 26: Galaxies: Interactions and Induced Star Formation Dynamics of Galaxy Interactions. pp 275–+
Barnes J. E., 2002, MNRAS, 333, 481
Bekki K., 1998, ApJ, 502, L133+
Bell E. F., Naab T., McIntosh D. H., Somerville R. S., Caldwell J. A. R., Barden M., Wolf C., Rix H.-W., Beckwith S. V. W., Borch A., Haeussler B., Heymans C., Jahnke K., Jogee S., Meisenheimer K., Peng C. Y., Sanchez S. F., Wisotzki L., 2005, ArXiv Astrophysics e-prints
Binggeli B., Jerjen H., 1998, A&A, 333, 17
Binney J., 2005, ArXiv Astrophysics e-prints
Bournaud F., Combes F., Jog C. J., 2004, A&A, 418, L27
Bournaud F., Jog C. J., Combes F., 2005, A&A, 437, 69
Burkert A., 1993, A&A, 278, 23
Burkert A., Naab T., 2005, ArXiv Astrophysics e-prints
Caon N., Capaccioli M., D'Onofrio M., 1993, MNRAS, 265, 1013
Caon N., Capaccioli M., D'Onofrio M., 1994, A&AS, 106, 199
Caon N., Capaccioli M., Rampazzo R., 1990, A&AS, 86, 429
Capaccioli M., 1987, in IAU Symp. 127: Structure and Dynamics of Elliptical Galaxies Distribution of light - Outer regions. pp 47–60
Carlberg R. G., 1986, ApJ, 310, 593
Cox T. J., Jonsson P., Primack J. R., Somerville R. S., 2005, ArXiv Astrophysics e-prints
Davies J. I., Phillipps S., Cawson M. G. M., Disney M. J., Kibblewhite E. J., 1988, MNRAS, 232, 239
de Jong R. S., Simard L., Davies R. L., Saglia R. P., Burstein D., Colless M., McMahan R., Wegner G., 2004, MNRAS, 355, 1155
de Vaucouleurs G., 1948, Annales d'Astrophysique, 11, 247
Freeman K. C., 1970, ApJ, 160, 811
González-García A. C., Balcells M., 2005, MNRAS, 357, 753
González-García A. C., van Albada T. S., 2005, MNRAS, 361, 1043
Graham A., Lauer T. R., Colless M., Postman M., 1996, ApJ, 465, 534
Graham A. W., 2001, MNRAS, 326, 543
Graham A. W., Erwin P., Caon N., Trujillo I., 2001, ApJ, 563, L11
Graham A. W., Trujillo I., Caon N., 2001, AJ, 122, 1707
Gutiérrez C. M., Trujillo I., Aguerri J. A. L., Graham A. W., Caon N., 2004, ApJ, 602, 664
Hernquist L., 1990, ApJ, 356, 359
Hernquist L., 1992, ApJ, 400, 460
Hernquist L., 1993a, ApJS, 86, 389
Hernquist L., 1993b, ApJ, 409, 548
Heyl J. S., Hernquist L., Spergel D. N., 1994, ApJ, 427, 165
Jerjen H., Binggeli B., 1997, in ASP Conf. Ser. 116: The Nature of Elliptical Galaxies; 2nd Stromlo Symposium Are "Dwarf" Ellipticals Genuine Ellipticals?. pp 239–+
Jesseit R., Naab T., Burkert A., 2005, MNRAS, 360, 1185
Jog C. J., Chitre A., 2002, A&A, 393, L89
Kawai A., Fukushige T., Makino J., Taiji M., 2000, PASJ, 52, 659
Khochfar S., Burkert A., 2006, A&A, 445, 403
Labbé I., Rudnick G., Franx M., Daddi E., van Dokkum P. G., Förster Schreiber N. M., Kuijken K., Moorwood A., Rix H.-W., Röttgering H., Trujillo I., van der Wel A., van der Werf P., van Starkenburg L., 2003, ApJ, 591, L95
Merritt D., Navarro J. F., Ludlow A., Jenkins A., 2005, ApJ, 624, L85
Mihos J. C., Hernquist L., 1996, ApJ, 464, 641
Naab T., Burkert A., 2001a, in ASP Conf. Ser. 230: Galaxy Disks and Disk Galaxies Gas Dynamics and Disk Formation in 3:1 Mergers. pp 451–452
Naab T., Burkert A., 2001b, ApJ, 555, L91
Naab T., Burkert A., 2003, ApJ, 597, 893
Naab T., Burkert A., Hernquist L., 1999, ApJ, 523, L133
Naab T., Johansson P. H., Efstathiou G., Ostriker J. P., 2005, ArXiv Astrophysics e-prints
Naab T., Khochfar S., Burkert A., 2006, ApJ, 636, L81
Naab T., Ostriker J. P., 2006, MNRAS, pp 94–+
Ostriker J. P., 1980, Comments on Astrophysics, 8, 177
Peletier R. F., Davies R. L., Illingworth G. D., Davis L. E., Cawson M., 1990, AJ, 100, 1091
Pierce M. J., Tully R. B., 1992, ApJ, 387, 47
Press W. H., Teukolsky S. A., Vetterling W. T., Flannery B. P., 1992, Numerical recipes in FORTRAN. The art of scientific computing. Cambridge: University Press, —c1992, 2nd ed.
Prugniel P., Simien F., 1997, A&A, 321, 111
Rix H., Carollo C. M., Freeman K., 1999, ApJ, 513, L25
Rix H., Franx M., Fisher D., Illingworth G., 1992, ApJ, 400, L5
Robertson B., Cox T. J., Hernquist L., Franx M., Hopkins P. F., Martini P., Springel V., 2005, ArXiv A e-prints
Rothberg B., Joseph R. D., 2004, AJ, 128, 2098
Rubin V. C., Graham J. A., Kenney J. D. P., 1992, ApJ, 394, L9
Sersic J. L., 1968, Atlas de galaxias australes. Cordoba, Argentina: Observatorio Astronomico, 1968
Springel V., Di Matteo T., Hernquist L., 2005, ApJ, 620, L79
Springel V., Hernquist L., 2005, ApJ, 622, L9
Trujillo I., Aguerri J. A. L., Gutiérrez C. M., Cepa J., 2001, AJ, 122, 38
Trujillo I., Burkert A., Bell E. F., 2004, ApJ, 600, L39
Vazdekis A., Trujillo I., Yamada Y., 2004, ApJ, 601, L33
Weil M. L., Hernquist L., 1996, ApJ, 460, 101
Young C. K., Currie M. J., 1994, MNRAS, 268, L11+
Young C. K., Currie M. J., 1995, MNRAS, 273, 1141